AD-A136 289 LEAST FAVORABLE RESPONSE OF INELASTIC STRUCTURES(U) NEW MEXICO UNIV ALBUQUERQUE BUREAU OF ENGINEERING RESEARCH F C CHANG ET AL. MAR 83 CE-63(83)AFOSR-993-1 1/1

UNCLASSIFIED AFOSR-TR-83-1226 AFOSR-81-0086 F/G 20/11 NL

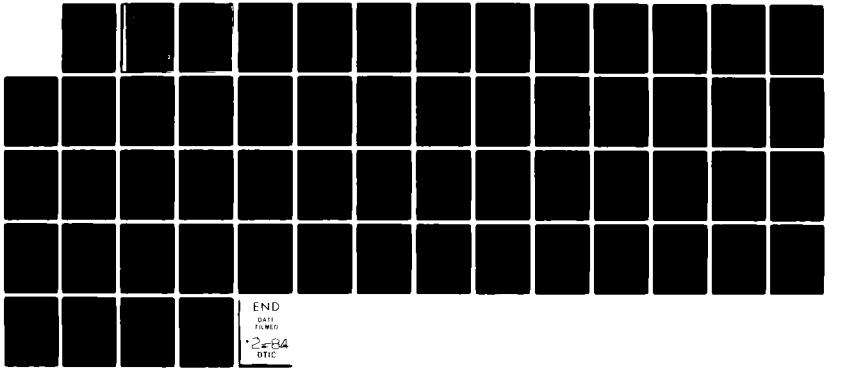

END

DATE FILMED

2-84

DTIC

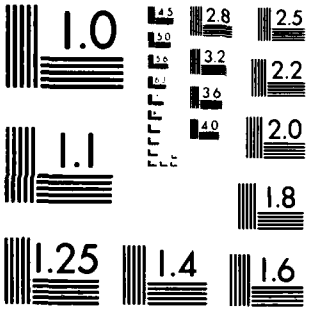

MICROCOPY RESOLUTION TEST CHART
NATIONAL BUREAU OF STANDARDS 1963 A

AFOSR-TR- 83 - 1226

A136289

THE UNIVERSITY OF NEW MEXICO
COLLEGE OF ENGINEERING

BUREAU OF ENGINEERING RESEARCH

DTIC FILE COPY

LEAST FAVORABLE RESPONSE OF INELASTIC STRUCTURES

by

Fashin Craig Chang

Thomas L. Paez

Frederick Ju

Technical Report CE-63(83)AFOSR-993-1

March 1983

Work performed under
Contract No. 81-0086. AFOSR-81-0086

DTIC
ELECTE
DEC 23 1983
S D
A

Approved for Public Release; Distribution Unlimited.

83 12 22 020

Qualified requestors may obtain additional copies from
the Defense Technical Information Service.

Reproduction, translation, publication, use and disposal
in whole or in part by or for the United States Government
is permitted.

UNCLASSIFIED

SECURITY CLASSIFICATION OF THIS PAGE (When Data Entered)

REPORT DOCUMENTATION PAGE		READ INSTRUCTIONS BEFORE COMPLETING FORM
1. REPORT NUMBER AFOSR-TR- 83-1226	2. GOVT ACCESSION NO. AD-A136289	3. RECIPIENT'S CATALOG NUMBER
4. TITLE (and Subtitle) LEAST FAVORABLE RESPONSE OF INELASTIC STRUCTURES		5. TYPE OF REPORT & PERIOD COVERED INTERIM
		6. PERFORMING ORG. REPORT NUMBER
7. AUTHOR(s) FASHIN CRAIG CHANG THOMAS L PAEZ FREDERICK JU		8. CONTRACT OR GRANT NUMBER(s) AFOSR-81-0086
9. PERFORMING ORGANIZATION NAME AND ADDRESS UNIVERSITY OF NEW MEXICO BUREAU OF ENGINEERING RESEARCH ALBUQUERQUE, NM 87131		10. PROGRAM ELEMENT, PROJECT, TASK AREA & WORK UNIT NUMBERS 61102F 2307/C2
11. CONTROLLING OFFICE NAME AND ADDRESS AIR FORCE OFFICE OF SCIENTIFIC RESEARCH/NA BOLLING AFB, DC 20332		12. REPORT DATE March 1983 13. NUMBER OF PAGES 55
14. MONITORING AGENCY NAME & ADDRESS(if different from Controlling Office)		15. SECURITY CLASS. (of this report) Unclassified 15a. DECLASSIFICATION/DOWNGRADING SCHEDULE

16. DISTRIBUTION STATEMENT (of this Report)

Approved for Public Release; Distribution Unlimited.

17. DISTRIBUTION STATEMENT (of the abstract entered in Block 20, if different from Report)

18. SUPPLEMENTARY NOTES

19. KEY WORDS (Continue on reverse side if necessary and identify by block number)

shock	inelastic structures	peak response
vibration	least favorable response	energy dissipation
testing	least favorable input	

20. ABSTRACT (Continue on reverse side if necessary and identify by block number)

In the design of a structural system, a test input is sought to conservatively represent an ensemble of measured field inputs. When a structure survives the test input, it is assumed that it would survive the field inputs. The method of shock response spectra is a technique for specifying conservative test inputs, but it has some disadvantages. In this investigation a technique is developed for the specification of test inputs. It is based on the method of least favorable response, and it overcomes some of the shortcomings of the method of shock response spectra. Numerical examples show that the present technique can be used in practical applications.

DD FORM 1 JAN 73 1473 EDITION OF 1 NOV 65 IS OBSOLETE

UNCLASSIFIED

SECURITY CLASSIFICATION OF THIS PAGE (When Data Entered)

LEAST FAVORABLE RESPONSE OF INELASTIC STRUCTURES

by

Fashin Craig Chang

Thomas L. Paez

Frederick Ju

The University of New Mexico

(Department of Civil Engineering
and
Department of Mechanical Engineering)

Technical Report CE-63(83)AFOSR-993-1

Chief, Information Division

March 1983

ACKNOWLEDGEMENT

The authors wish to acknowledge the support of the Air Force office of Scientific Research in this study. The work was performed under AFOSR contract number 81-0086.

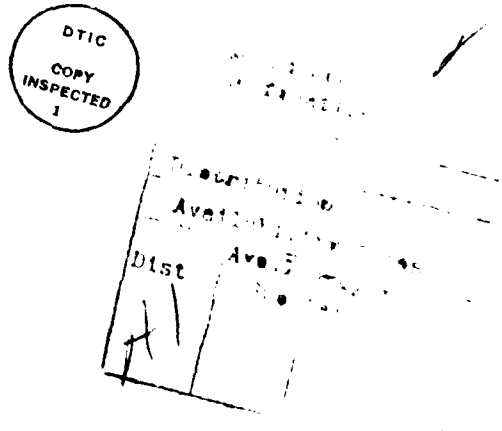

ABSTRACT

In the design of a structural system, a test input is sought to conservatively represent an ensemble of measured field inputs. When a structure survives the test input, it is assumed that it would survive the field inputs. The method of shock response spectra is a technique for specifying conservative test inputs, but it has some disadvantages. In this investigation a technique is developed for the specification of test inputs. It is based on the method of least favorable response, and it overcomes some of the shortcomings of the method of shock response spectra. Numerical examples show that the present technique can be used in practical applications.

TABLE OF CONTENTS

LIST OF FIGURES

LIST OF TABLES

1.0 Introduction

In the design of a structural system the engineer attempts to provide a plan for a structure that will survive one or more input excitations. To do this the engineer must have some means for analyzing structural response, and for judging whether the system can survive an excitation or a class of excitations. Most realistic situations involve environments that are random, and in such cases design techniques are sought to specify structures with preestablished probabilities of failure.

Short duration, strong motion excitations excite extreme responses, and structural failure can occur due to peak response; consequently it is desirable to know what maximum response can be caused in a structural system by a dynamic load. For reasons of conservatism and design safety, it is desirable to establish a procedure for computing a bound on the maximum structural response caused by a shock input. Buildings designed to survive an upper bound on the peak response should respond satisfactorily to the actual input.

A structural input excitation used in an analysis or physical test is considered conservative if it excites a more severe response in a structure than the individual inputs it is meant to represent. Therefore, when measured environments representing a real shock source are available, and it is necessary to design a structure to survive that source, a conservative input representing the measured shock is sought.

The method of shock response spectra provides a technique for the analysis and design of structures subjected to short duration shock excitations. The method of shock response spectra is used to establish a test input that can represent an ensemble of inputs conservatively, in the sense that the peak response excited by the test input is greater than the peak response

excited by any of the underlying measured inputs. References 1 through 5 provide reviews and some recent applications of the method of shock response spectra in structural analysis and design.

The method of shock response spectra attempts to represent an ensemble of shock signals in a conservative way and bounds the effects of a collection of shocks in a peak response sense. Since shocks are usually considered random, and a shock test specified using the method of shock response spectra depends on an ensemble of measured shocks, the shock test has only some non-unit probability of being conservative. In general, this probability is unknown.

The method of least favorable response was established by Drenick and Shinozuka in References 6 and 7. Its applicability was extended to use in analytical and physical testing by Witte and Wolf in Reference 8. The method of least favorable response provides an alternate method for the specification of test inputs. The technique allows the engineer to specify a test input based on an ensemble of measured shock inputs. The test input will cause a response in a linear structure that is a bound on the response excited by the underlying measured inputs. Therefore, this method is equivalent, in concept, to the method of shock response spectra. Reference 9 compares the methods of least favorable response and shock response spectra and shows that the former has some considerable advantages over the latter.

There are many other methods available for the specification of shock tests. Any analytical technique which permits the definition of a structural response bound based on an underlying ensemble of inputs can be used to establish a shock test specification method. Papers by Youssef and Popplewell (References 10, 11, 12) and Papoulis (Reference 13) show how some bounds can be

established, and these approaches could be used as the basis for shock test specifications.

One of the main disadvantages of the methods discussed above is that shock environments are often represented using test inputs that are different in character from the original shocks. This problem is discussed in detail by Baca in Reference 14. He shows that this problem can lead to overconservative tests, especially in the case of the method of shock response spectra where simple waveform test inputs can be used.

Another disadvantage is that the techniques discussed above are mainly for use with linear structures. Of course, the techniques are used in connection with failure analysis of structures, but the theoretical developments are usually concerned with linear equations. One exception occurs with the method of shock response spectra; a few papers concerned with test specification for nonlinear structures have been written. (See, for example, References 15, 16, 17.)

Beyond the two problems mentioned above, it is certainly clear that not all failures are related simply to the peak response of a structure. Damage may accumulate in a structure due to vibratory cycling in the response, and this may lead to failure. For example, References 18 and 19 refer to the accumulation of damage in this manner. And Reference 20 summarizes the results of experiments on concrete that demonstrate how the accumulation of damage is related to the energy dissipated in a test specimen.

In view of these problem areas, it is desirable to develop a technique for the specification of test inputs for the analysis and design of structures that 1) yields inputs similar in form to the underlying measured inputs, 2) accounts for the potential for nonlinear response in a structure, and 3) can be used when failure is related to peak response or accumulation of damage.

The objective of this study is to establish a method for the specification of a test input based on an ensemble of measured inputs. The input will have the three properties listed in the previous paragraph. The approach is based on the method of least favorable response; therefore, the linear theory of least favorable response is reviewd in the following section. Next, the peak reponse of bilinear hysteretic single-degree-of-freedom (SDF) structures is investigated. The peak value of energy dissipated in a structural system is then studied. Finally, a method is established for specifying a test input that will cause maximum displacement response or maximum energy dissipation in a structure.

2.0 The Linear Theory of Least Favorable Response

The method of least favorable response provides a means for defining an upper bound on the response of a linear structure excited by a sequence of shock inputs. Consider a linear dynamical structure. When it is excited by a single input, the response at a point on the structure can always be expressed using the convolution integral. This is

$$y(t) = \int_{-\infty}^{\infty} h(t - \tau)\, x(\tau) d\tau \qquad (2\text{-}1)$$

where $x(t)$ is the input excitation, $y(t)$ is the response, and $h(t)$ is the system impulse response function. If the system response starts at time zero, then it is assumed that the initial conditions are zero velocity and displacement.

Now assume that the structure has positive viscous damping and the input can be Fourier transformed. Then the response has a Fourier transform, and the input and response Fourier transforms are given by

$$X(\omega) = \int_{-\infty}^{\infty} x(t)\, e^{-i\omega t}\, dt \qquad (2\text{-}2)$$

$$Y(\omega) = \int_{-\infty}^{\infty} y(t)\, e^{-i\omega t}\, dt \qquad (2\text{-}3)$$

These functions possess inverse Fourier transforms and these are given by

$$x(t) = \frac{1}{2\pi} \int_{-\infty}^{\infty} X(\omega)\, e^{i\omega t}\, d\omega \qquad (2\text{-}4)$$

$$y(t) = \frac{1}{2\pi} \int_{-\infty}^{\infty} Y(\omega)\, e^{i\omega t}\, d\omega \qquad (2\text{-}5)$$

The convolution integral in Equation (2-1) can be Fourier transformed. The result is

$$Y(\omega) = H(\omega)\ X(\omega) \tag{2-6}$$

where H(w) is the Fourier transform of the impulse response function. That is

$$H(\omega) = \int_{-\infty}^{\infty} h(t)\ e^{-i\omega t}\ dt \tag{2-7}$$

The inverse Fourier transform of this function is

$$h(t) = \frac{1}{2\pi} \int_{-\infty}^{\infty} H(\omega)\ e^{i\omega t}\ d\omega \tag{2-8}$$

When Equation (2-6) is used in Equation (2-5), a frequency domain exprssion is obtained for the structural response. This is

$$y(t) = \frac{1}{2\pi} \int_{-\infty}^{\infty} H(\omega)\ X(\omega)\ e^{i\omega t}\ d\omega \tag{2-9}$$

The objective is to bound the maximum value in the absolute value of the response; therefore, the absolute value is taken in Equation (2-9). This yields

$$\left|y(t)\right| = \frac{1}{2\pi} \left| \int_{-\infty}^{\infty} H(\omega)\ X(\omega)\ e^{i\omega t}\ d\omega \right| \tag{2-10}$$

An inequality of calculus can be used to show that when the absolute value signs are taken inside the integral on the right, above, the absolute value of the response is bounded, as follows.

$$\left|y(t)\right| \leq \frac{1}{2\pi} \int_{-\infty}^{\infty} \left|H(\omega)\right| \left|X(\omega)\right|\ d\omega = I \tag{2-11}$$

The expression on the right is a constant, independent of time; this constant is denoted I. Since the absolute value of the response is equal to or less than I, this implies that the maximum value in the absolute value of the response is equal to or less than I. Let

$$Y = \max_t |y(t)|, \tag{2-12}$$

then

$$Y \leq I \tag{2-13}$$

The quantity, I, is known as the least favorable response (LFR) of the system, corresponding to the input with Fourier transform given by Equation (2-2). The LFR forms a bound on all the peak responses of the system whose frequency response function is $H(\omega)$ where the input has Fourier transform modulus bounded by $|X(\omega)|$. A test input is known as a least favorable input (LFI) if it produces a response whose absolute maximum is equal to I.

Let $X_T(t)$ denote a test input with Fourier transform $X_T(\omega)$. This input excites a response $y_T(t)$, in the system of interest, whose Fourier transform is $Y_T(\omega) = H(\omega)X_T(\omega)$. A bound on the absolute maximum of the test response is given by

$$\max_t |y_T(t)| = \frac{1}{2\pi} \int_{-\infty}^{\infty} |X_T(\omega)||H(\omega)| \, d\omega \tag{2-14}$$

The Fourier transforms of the test input, $X_T(\omega)$, and the frequency response function can be expressed in their polar forms.

$$X_T(\omega) = |X_T(\omega)| \, e^{i\theta_T(\omega)} \tag{2-15}$$

$$H(\omega) = |H(\omega)| \, e^{i\phi(\omega)} \tag{2-16}$$

When the expressions are used in Equation 2-9, the response function $y_T(t)$ is given by

$$y_T(t) = \frac{1}{2\pi}\int_{-\infty}^{\infty} |X_T(\omega)||H(\omega)|\, e^{i(\theta_T(\omega) + \phi(\omega) - \omega t)}\, d\omega \quad (2\text{-}17)$$

At time t = 0, the above expression can be made equal to I, the LFR, by taking

$$\theta_T(\omega) = -\phi(\omega) \quad (2\text{-}18)$$

and

$$X_T(\omega) = |X(\omega)| \quad (2\text{-}19)$$

In this case the test response at time zero is

$$y_T(0) = \frac{1}{2\pi}\int_{-\infty}^{\infty} |X(\omega)||H(\omega)|\, d\omega = I \quad (2\text{-}20)$$

This shows that the test response can be made equal to the LFR by choosing the Fourier transform modulus of the test input equal to the Fourier transform modulus of the actual input, and by choosing the complex phase of the test input equal to minus the phase of the frequency response function. The effect of this choice of phase is to cause the response Fourier components to add constructively at time t = 0.

In view of Equations 2-18 and 2-19 the Fourier transform of the test input is given by

$$X_T(\omega) = |X(\omega)|\, e^{-i\phi(\omega)} \quad (2\text{-}21)$$

This function can be inverse Fourier transformed to obtain a time domain espression for the test input. This input is the LFI.

$$x_T(t) = \frac{1}{2\pi} \int_{-\infty}^{\infty} X_T(\omega)\ e^{i\omega t}\ d\omega \qquad (2\text{-}22)$$

This input could be used in a physical test of the structure. Since the response it excites is equal to or greater than the response excited by the input X(t), the test input produces a conservative test, in the peak response sense. If a structure survives $x_T(t)$, then it would also survive x(t).

The procedure outlined above provides a means for computing the LFR and specifying a shock test based on one measured input, x(t). The procedure can be modified to define an LFR and shock test input when several measured inputs are available. Let $x_j(t)$, j=1,...n, be a sequence of measured shock signals from one or more shock sources, and assume that a structure of interest will be subjected to one or more shocks from each source in the field. Then an LFR based on the sequence of inputs can be constructed as follows. Compute the Fourier transform of each shock and denote the results $X_j(\omega)$, j=1,...n. Compute the complex modulus of each Fourier transformed signal, $|X_j(\omega)|$, j=1,...n. Let $X_e(\omega)$ define the envelope of the Fourier transformed moduli; then $X_e(\omega)$ is

$$X_e(\omega) = \max_j |X_j(\omega)| \qquad (2\text{-}23)$$

The LFR based on the sequence of inputs is given by

$$I = \frac{1}{2\pi} \int_{-\infty}^{\infty} X_e(\omega)\ |H(\omega)|\ d\omega \qquad (2\text{-}24)$$

This is a bound on the peak response excited by the inputs, $x_j(t)$,j=1,...n, individually, since $X_e(\omega)$ bounds the Fourier transform moduli of the individual inputs.

A test input which will excite the LFR, at time t = 0, is given by

$$X_T(t) = \frac{1}{2\pi} \int_{-\infty}^{\infty} X_e(\omega) \left|H(\omega)\right| e^{i\omega t} \, d\omega \qquad (2\text{-}25)$$

This input could be used in a physical test of the structure. It is conservative with respect to each of the individual inputs in a peak response sense.

The method of least favorable response has a few features that make it practically important. First, it generates test inputs and responses that are convservative with respect to a collection of underlying inputs and the responses they excite. Second, it generates test inputs that have the same oscillatory quality as the underlying inputs. Third, it preserves the power of the underlying input by matching $X_e(\omega)$ to the moduli of the Fourier transforms of the underlying inputs and simply rearranging the phase of the response.

3.0 A Displacement Response Bound for Bilinear Hysteretic Systems

It was shown in Section 2.0 that for a linear system the least favorable response (LFR) can be obtained from Equation 2-14. The LFR is a bound on the individual responses excited by a sequence of inputs. The least favorable input (LFI) given in Equation 2-25 is a test input which generates the LFR in a linear system. In this section a technique is developed to compute the LFR of a nonlinear single-degree-of-freedom (SDF) structure.

The capacity to generate the LFR of an SDF structure is important since it can be used by the designer to establish a bound on the displacement response of a multi-degree-of-freedom (MDF) structure in its fundamental mode. In many practical cases the fundamental mode of response contributes most significantly to the overall response. Beyond this, the results of this investigation may prove useful for application in the definition of inputs at several characteristic frequencies, simultaneously.

The technique to be considered is based on the method of least favorable response. The LFI is an input characterized in terms of the complex modulus and phase of its Fourier transform. The modulus of the Fourier transform of an LFI reflects an envelope on the moduli of the Fourier transforms of the underlying inputs. When the shock sources represented in the ensemble of inputs are very similar, then the moduli of the Fourier transforms of the inputs are very similar and the envelope very nearly matches these. The complex phase functions of the Fourier transforms of actual inputs are random, at least in part. And the complex phase of the Fourier transform of the LFI is chosen to cause the components of the response to superpose constructively at time $t = 0$. The phase is chosen as minus the complex phase of the frequency response function of the structure under consideration.

In this investigation it is assumed that the bilinear hysteretic structure possesses an LFR and an LFI which generates that response. It is assumed that the LFI of the bilinear system has the same general form as the LFI of the linear system. The parameters of this LFI must be determined.

Consider a base excited, linear SDF system. The frequency response function for the system is given by

$$H(\omega) = \frac{1}{(\omega_n^2 - \omega^2) + 2\, i\zeta\, \omega_n \omega} \qquad -\infty < \omega < \infty \qquad (3\text{-}1)$$

where ω_n is the natural frequency of the system and ζ is the damping factor of the system. This function can be interpreted in terms of its real and imaginary parts or its complex modulus and phase. The phase of the frequency response function is

$$\phi(\omega) = \tan^{-1} \frac{-2\zeta\omega_n\omega}{\omega_n^2 - \omega^2}, \qquad -\infty < \omega < \infty \qquad (3\text{-}2)$$

This is plotted in Figure 3.1 as a function of circular frequency, ω. Note that $\phi(\omega)$ is an odd function and varies rapidly in the vicinity of ω_n and slowly elsewhere.

It is assumed in this study that the complex phase of the Fourier transform of the LFI of a bilinear hysteretic system is given by

$$\phi(\omega) = \tan^{-1} \frac{-2\zeta_e\omega_e\omega}{\omega_e^2 - \omega^2}, \qquad -\infty < \omega < \infty \qquad (3\text{-}3)$$

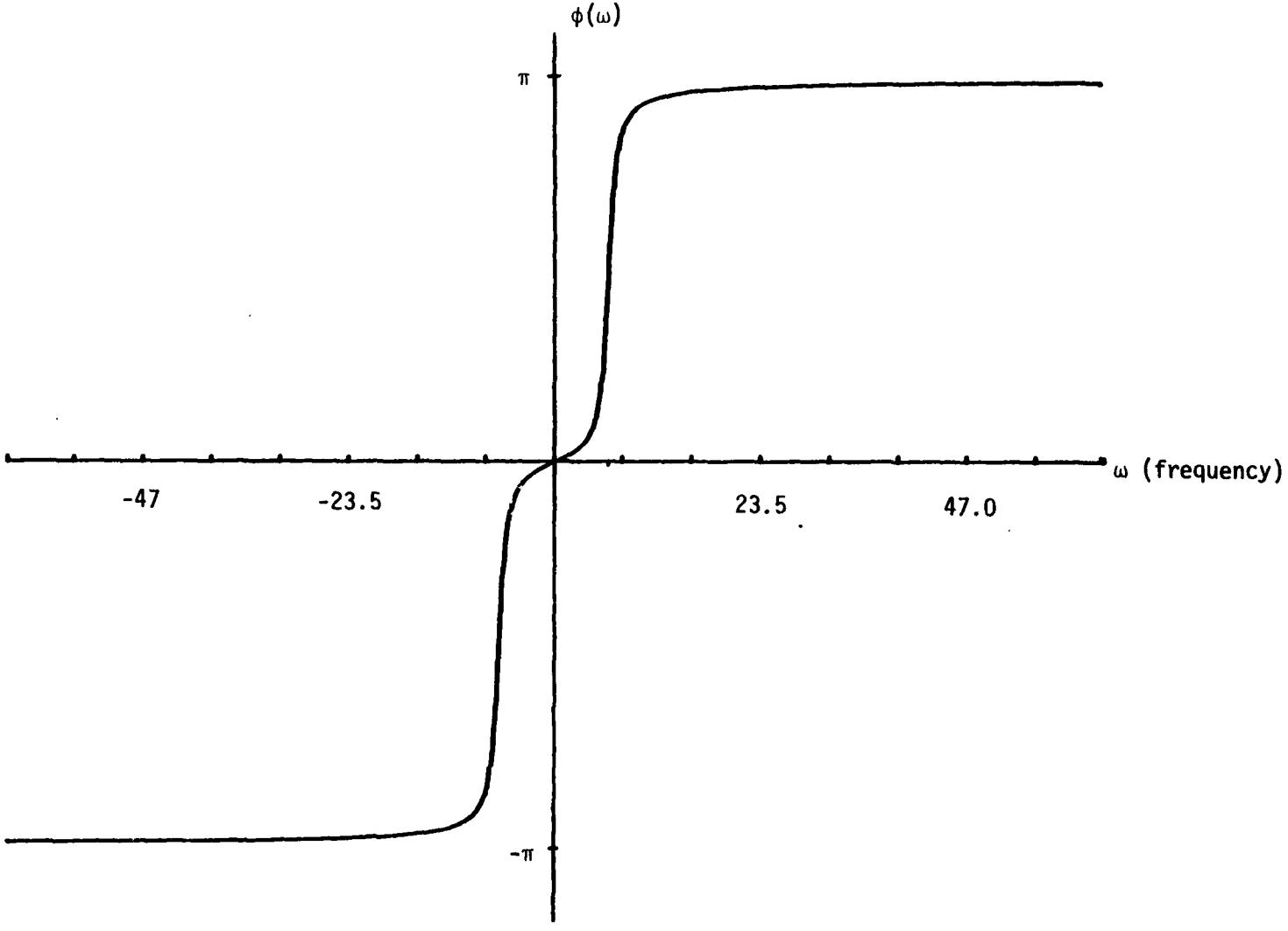

Figure 3.1. Complex Phase of SDF System Frequency Response Function, $\omega_n = 2\pi$

where ω_e is the characteristic frequency and ζ_e is the characteristic damping factor. These parameters are chosen to maximize the response of the bilinear system. The parameters must be determined.

For a specific bilinear hysteretic system and ensemble of inputs, the parameters in the phase of the Fourier transform of the LFI can be determined by searching the peak response values as a function of ω_e and ζ_e to obtain a maximum. The response of a bilinear hysteretic SDF system is governed by the equation

$$\ddot{y} + 2\zeta\omega_n \dot{y} + \frac{1}{m} R(y) = -\ddot{x}_0 \qquad (3\text{-}4)$$

where ζ and ω_n are the damping factor and small displacement natural frequency of the system, m is the SDF system mass, $\ddot{x}_0$ is the base motion input excitation of the system, R(y) is the bilinear hysteretic restoring force function. The restoring force is a function with an infinite number of realizations. When y is small, R(y) is a linear function of y with stiffness k. When the yield displacement, D, is surpassed, then permanent set accumulates in the system and the stiffness reduces to k_y. When the velocity reverses sign the stiffness increases to k and oscillations occur about a new equilibrium displacement (reflecting the permanent set) until yielding occurs again, etc. Figure 3-2 shows a potential realization of the spring restoring force function for a bilinear hysteretic system. Equation 3-4 can be solved using a numerical procedure. For example, the numerical procedure given in Reference 21 can be used to solve Equation 3-4.

Let $x_j(t)$, j=1,...n be an ensemble of measured inputs from one or more shock sources to which a structure will be exposed. The LFR and LFI of a bilinear hysteretic structure corresponding to these inputs are defined as follows. Compute the Fourier transforms of the inputs and denote these $X_j(\omega)$, j=1,...n.

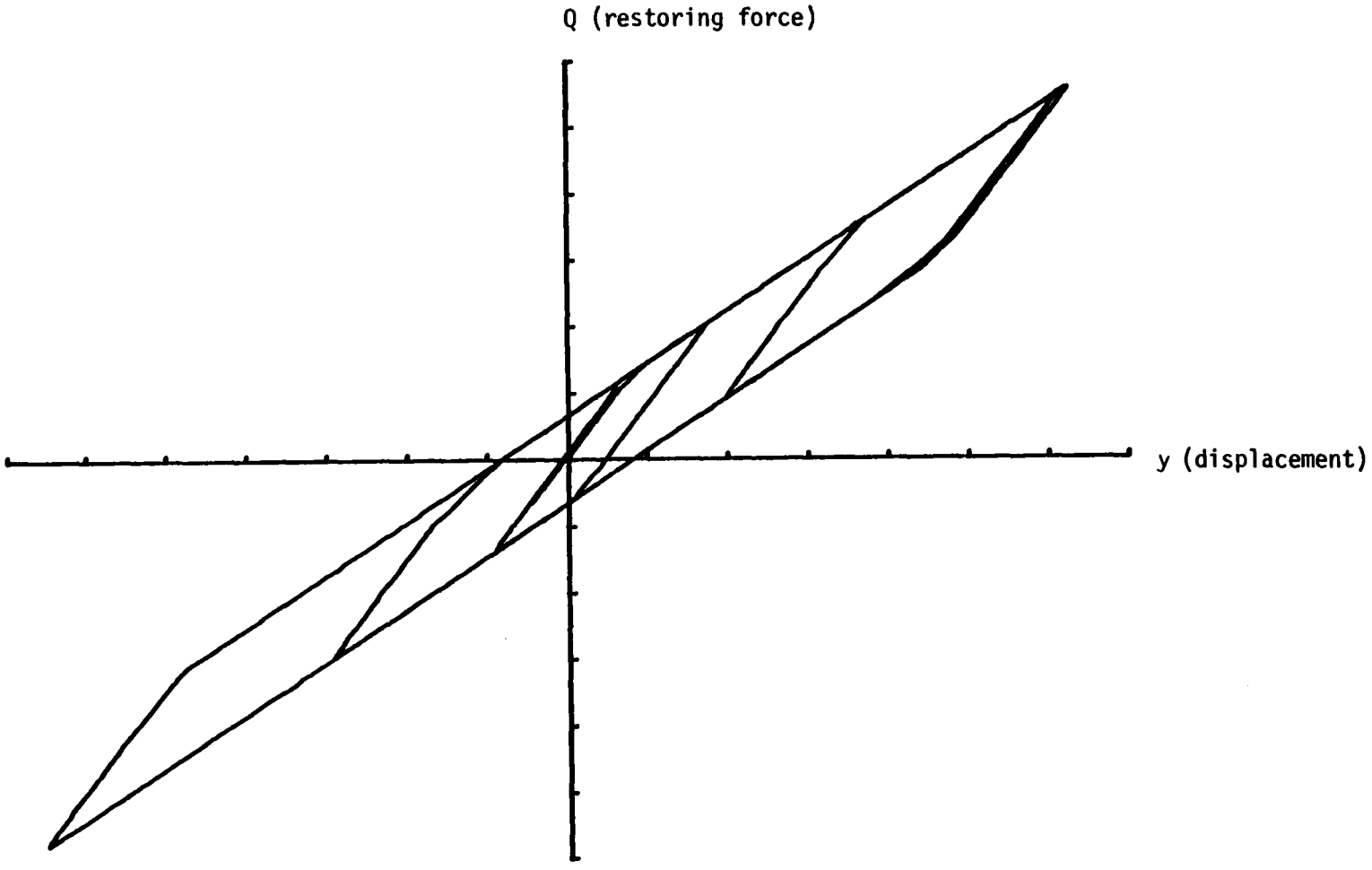

Figure 3.2. Realization of Restoring Force Function of Bilinear Hysteretic Spring

Then compute the complex moduli of the inputs and find the envelope of the moduli. This is

$$X_e(\omega) = \max_j |X_j(\omega)| \quad -\infty < \omega < \infty \tag{3-5}$$

This is the modulus of the Fourier transform of the LFI. The form of the complex phase of the LFI is given in Equation 3-3. When specific values of ω_e and ζ_e are used in Equation 3-3, an input whose Fourier transform has the form of the LFI can be established. This is

$$X_T(\omega) = X_e(\omega) \exp\left[i \tan^{-1} \left[\frac{-2\zeta_e \omega_e \omega}{\omega_e^2 - \omega^2} \right] \right], \quad -\infty < \omega < \infty \tag{3-6}$$

A time domain test input can be established by inverse Fourier transforming this function. The result is

$$x_T(t) = \frac{1}{2\pi} \int_{-\infty}^{\infty} X_T(\omega)\, e^{i\omega t}\, d\omega, \quad -\infty < t < \infty \tag{3-7}$$

This function of time can be used as input in Equation 3-4 and the response can be computed numerically and denoted $y_T(t, \omega_e, \zeta_e)$. Dependence of the response function on the parameters of the input is emphasized by inclusion of these parameters as arguments in the response expression.

The peak value, in time, of the response is

$$Y(\omega_e, \zeta_e) = \max_t \left| y_T(t, \omega_e, \zeta_e) \right| \tag{3-8}$$

The peak response can be maximized with respect to ω_e and ζ_e by solving for the values of ω_e and ζ_e which satisfy the following equations.

$$\frac{\partial Y}{\partial \omega_e} = 0, \quad \frac{\partial Y}{\partial \zeta_e} = 0 \tag{3-9}$$

Denote the solution to these equations ω_e^* and ζ_e^*. Use of these values in Equations 3-7 yields the LFI. Evaluation of Equation 3-8 at $\omega_e = \omega_e^*$ and $\zeta_e = \zeta_e^*$ yields the LFR.

Equations 3-9 can be solved in any of a number of ways. In the present investigation they are solved using a simple search procedure.

4.0 An Energy Dissipation Bound for Bilinear Hysteretic Structures

Failure in structural systems is often related to execution of an extreme displacement response, and this potential is usually exploited in test specification techniques. However, other sources may contribute to the potential for failure. In many situations the accumulation of damage may lead to failure, even when the input and response are of short duration. In fact, the true criterion of failure depends in a complex way on both the damage accumulated in a system and the peak response it executes. In veiw of this, it is a matter of interest to specify test inputs that maximize accumulated damage when used to excite structures.

Many studies have considered the accumulation of structural damage. (See, for example, References 20, 22, and 23.) But there exists no universal measure of structural damage. It can safely be stated that the accumulation of damage is reflected by diminished strength or resistance in a structure. The experimental investigation in Reference 20 has shown that the energy dissipated by a structural material sample due to load cycling is related to the residual strength of the sample. Therefore, the amount of energy dissipated in a structural system can be related to structural damage.

In this section a method for specifying a test input based on an ensemble of measured inputs is established. The test input is characterized by the fact that it excites in a bilinear hysteretic system a response whose energy dissipated bounds the energy dissipated in the response excited by any of the inputs in the underlying ensemble. The test input has the same form as that used in the previous section. That is, the modulus of its Fourier transform envelops the moduli of the Fourier transforms of the inputs in the ensemble, and the phase of its Fourier transform is chosen to maximize the energy dissipated.

The system under investigation is governed by Equation 3-4 (repeated here for convenience).

$$\ddot{y} + 2\zeta\,\omega_n\,\dot{y} + \frac{1}{m}R(y) = -\ddot{x}_0 \qquad (4\text{-}1)$$

This system dissipates energy in two ways. It dissipates energy in the viscous damper, and it dissipates energy in the bilinear hysteretic spring. The total energy dissipated in the system can be expressed

$$E_T = E_D + E_s \qquad (4\text{-}2)$$

where E_D is the energy dissipated in the damper and E_s is the energy dissipated in the spring.

When the system response remains linear, no energy is dissipated in the spring and the entire energy dissipation in the system occurs in the damper. This is clearly so since a linear elastic spring does not dissipate energy. Beyond this, the amount of energy dissipated in the damper is independent of the phase of the input. This can be shown as follows. Note that the energy dissipated in the viscous damper is

$$E_D = \int_{y(-\infty)}^{y(\infty)} c\dot{y}\,dy \qquad (4\text{-}3)$$

where $y(-\infty)$ and $y(\infty)$ are the displacements at minus and plus infinity, and c is the system damping. This integral can be transformed to yield

$$E_D = \int_{-\infty}^{\infty} c\dot{y}^2\,dt \qquad (4\text{-}4)$$

Now since the system response considered here is linear, the displacement can be expressed using Equation 2-9 and the velocity response can be written using either of the following expressions:

$$\dot{y}(t) = \frac{1}{2\pi} \int_{-\infty}^{\infty} i\omega\, H(\omega)\, X(\omega)\, e^{i\omega t}\, d\omega \qquad (4\text{-}5a)$$

$$= -\frac{1}{2\pi} \int_{-\infty}^{\infty} i\omega\, H^*(\omega)\, X^*(\omega)\, e^{-i\omega t}\, d\omega$$

Both of the above expressions are correct since $\dot{y}(t)$ is a real function. When the term $\dot{y}^2$ in Equation 4-4 is written as $\dot{y} \cdot \dot{y}$ and Equations 4-5a and b are used, then Equation 4-4 becomes

$$E_D = \frac{c}{(2\pi)^2} \int_{-\infty}^{\infty} dt \int_{-\infty}^{\infty} d\omega_1 \int_{-\infty}^{\infty} d\omega_2\ \omega_1\omega_2\, H(\omega_1)H^*(\omega_2)X(\omega_1)X^*(\omega_2) \cdot e^{i(\omega_1-\omega_2)t} \qquad (4\text{-}6)$$

The dummy variables ω_1 and ω_2 have been used to avoid confusion in the two expressions for $\dot{y}(t)$. Now the order of integration can be changed in Equation 4-6, moving the t integral to the inside. Then

$$E_D = \frac{c}{(2\pi)^2} \int_{-\infty}^{\infty} d\omega_1 \int_{-\infty}^{\infty} d\omega_2\, H(\omega_1)\, H^*(\omega_2)\, X(\omega_1)\, X^*(\omega_2) \cdot \int_{-\infty}^{\infty} e^{i(\omega_1-\omega_2)t}\, dt \qquad (4\text{-}7)$$

It may be recognized that the inner integral is a delta function with value 2π and argument $\omega_1 - \omega_2$. Therefore, Equation 4-7 can be rewritten

$$E_D = \frac{c}{2\pi} \int_{-\infty}^{\infty} d\omega_1 \int_{-\infty}^{\infty} d\omega_2\, H(\omega_1)H^*(\omega_2)\, X\,(\omega_1)\, X^*(\omega_2)\, \delta(\omega_1 - \omega_2) \qquad (4\text{-}8)$$

where $\delta(\omega_1 - \omega_2)$ is the Dirac delta function with argument $\omega_1 - \omega_2$. The ω_2 integral can be evaluated to obtain

$$E_D = \frac{c}{2\pi} \int_{-\infty}^{\infty} |H(\omega_1)|^2 |X(\omega_1)|^2 d\omega_1 \qquad (4\text{-}9)$$

This integral depends only on the complex magnitude of the Fourier transform of the input, and not its phase. Therefore, the energy dissipated in the linear response of a structural system is independent of the phase of the input.

It can be concluded from the above analysis that an LFI based on energy dissipated does not exist for linear systems. This does not imply that an energy based LFI is nonexistent for inelastic systems. But if a dissipated energy LFI does exist for bilinear hysteretic systems, it is not clear whether it should be related to energy dissipated in both the damper and inelastic spring, or to energy dissipated in the spring alone.

The answer is related to the actual damage mechanism of the physical system. In this investigation damage is assumed to occur due to the motion in both the damper and the hysteretic spring. Therefore, an LFI maximizing the total energy dissipated is sought.

The total energy dissipated in the system is

$$E_s = \int_{y(-\infty)}^{y(\infty)} [c\dot{y} + R(y)]dy \qquad (4\text{-}10)$$

This quantity can be evaluated numerically during the response computation in the following way. When an input $\ddot{x}_0(t)$ is specified, Equation 4-1 can be solved numerically, marching out the solution in time. In the solution process values for y, $\dot{y}$

and $\ddot{y}$ and R[y(t)] are known at each time step. A change of variables can be executed and Equation 4-10 can be rewritten

$$E_T = \int_{-\infty}^{\infty} c\dot{y}(t) + R[y(t)] \quad \dot{y}(t)\, dt \tag{4-11}$$

This quantity can be incrementally computed using the results available at the end of each time step. This procedure yields the energy dissipated in the system.

When an ensemble of measured inputs is given by x_j (t), j=1,...n, let the form of the LFI be defined by Equation 3-7, where its Fourier transform is given in Equation 3-6. $X_e(\omega)$ is defined in Equation 3-5, and $\phi(\omega)$ is defined in Equation 3-3. When specific values of ω_e and ζ_e are used to generate the test input in Equation 3-7, and this input is used to excite the system in Equation 4-1, a specific response is executed. The system dissipates energy and this can be determined using Equation 4-11. Denote the dissipated energy $E_T(\omega_e, \zeta_e)$. The energy dissipated is maximized with respect to ω_e and ζ_e by solving for the values of ω_e and ζ_e which satisfy the equations

$$\frac{\partial E_T}{\partial \omega_e} = 0, \quad \frac{\partial E_T}{\partial \zeta_e} = 0 \tag{4-12}$$

Denote the solution to these equations w_e^* and ζ_e^*. Use of these values in Equation 3-7 yields the LFI related to energy dissipation. Evaluation of the expression $E_T(\omega_e, \zeta_e)$ at $\omega_e = \omega_e^*$ and $\zeta_e = \zeta_e^*$ yields the LFR in terms of energy dissipated.

5.0 Numerical Examples

In the previous sections methods for the approximate determination of the least favorable input (LFI) and least favorable response (LFR) of a bilinear hysteretic system were developed. A computer program has been written to execute the computations required to determine the LFI and LFR. The computer program is named LFIR and a listing of the program is provided in the Appendix. Some numerical examples are solved in this section using the computer program.

Two types of problems are solved. First, the LFI and the response it excites are determined for a single input applied to a single structural system. This is done using both the peak displacement and energy criteria. Second, the parameters of the complex phase of the LFI are determined for a sequence of increasingly severe inputs. This problem is solved for three bilinear hysteretic systems using both the peak displacement and energy criteria.

The type of input used in all cases is an oscillatory random input with decaying exponential amplitude. The input is denoted $x_0(t)$ and its specific form is given by

$$x_0(t) = e^{-\alpha t} \sum_{j=1}^{N} c_j \cos(\omega_j t - \phi_j), \quad 0 \leq t \leq T \qquad (5\text{-}1)$$

α is the amplitude decay rate of the input; N is the number of components in the input; c_j, j=1,...N, are the input amplitudes; ω_j, j=1,...N, are the frequencies where the input has power; ϕ_j, j=1,...N, are mutually independent, uniform random variables disributed on the internal $(-\pi,\pi)$. The input is an approximately normally distributed, nonstationary random process.

5.1 Example One

Consider the response of a bilinear hysteretic SDF structure, whose parameters are given in Table 5.1, to the shock input whose parameters are given in Table 5.2. The input is shown in

Table 5.1 Bilinear Hysteretic System Parameters

$m = 1.0$ mass	$c = 1.256$ damping
$k = (2\pi)^2$ stiffness	$D = 0.0813$ yield displacement
$k_y = 0.5$ yield stiffness	$\omega_n = 2\pi$ natural frequency

Table 5.2 Shock Input Parameters

$N = 30 \qquad \alpha = 0.628$

$C_j = 2.0 \quad j=1,\ldots30$

$\omega_j = 0.1 + 0.238(j-1) \quad j=1,\ldots30$

Figure 5.1; the response to the input is shown in Figure 5.2. Since the yield displacement is 0.0813, the response is clearly in the plastic region, in this example. The peak response caused by the actual input is 0.1651.

The LFI and LFR were computed using program LFIR. The parameters of the complex phase of the Fourier transform of the input were found to be $\omega_e = 5.056$ and $\zeta_e = 0.109$.

The modulus of the Fourier transform of the input is shown in Figure 5.3. The LFI, computed using Equation 3-7, is shown in Figure 5.3. The LFI, computed using Equation 3-7, is shown in Figure 5.4. The response excited by this input is shown in Figure 5.5. This time history shows that the LFI is 0.3012.

The LFI and LFR were also computed using the energy dissipation criterion. The energy dissipated during the response to the actual input is 0.1214. The parameters of the complex phase of

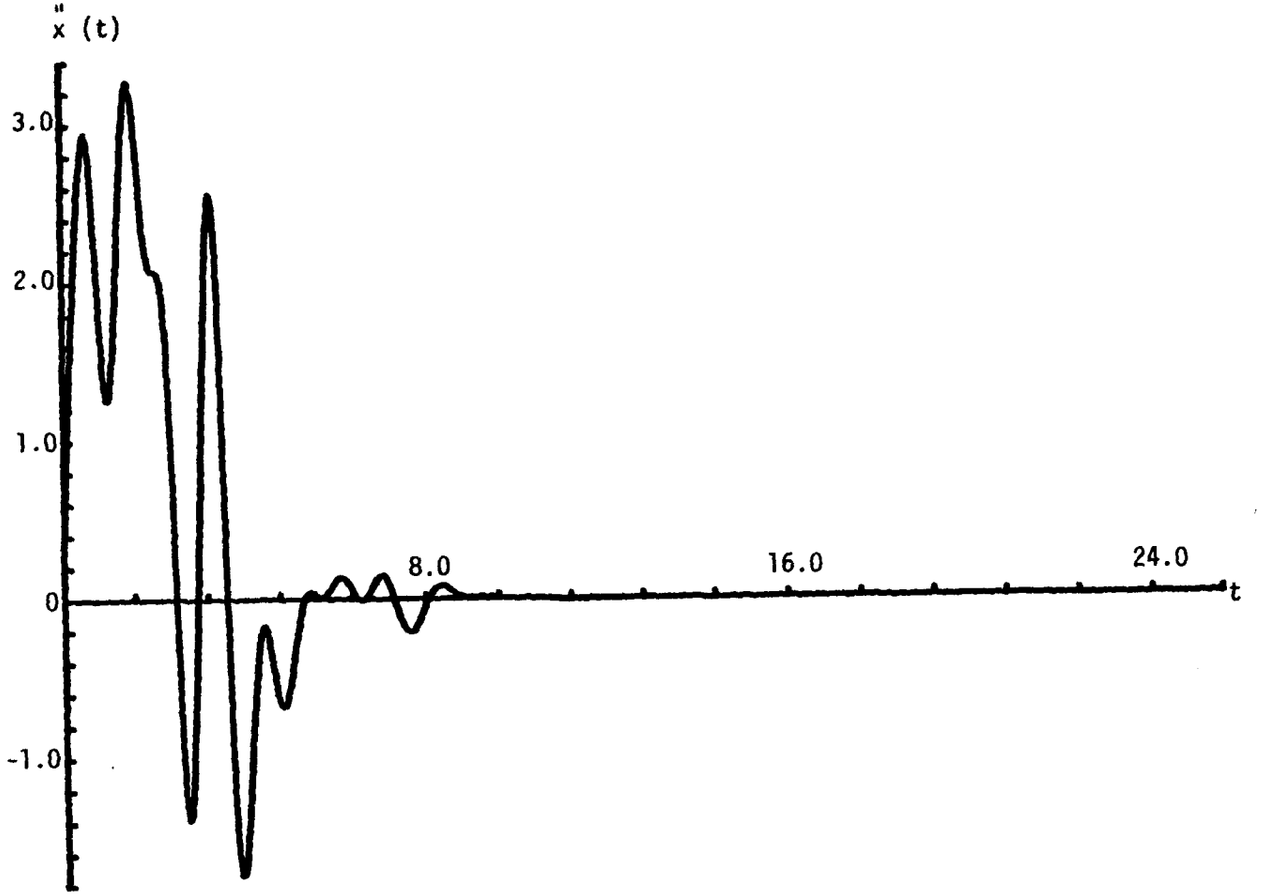

Figure 5.1. Input Time History

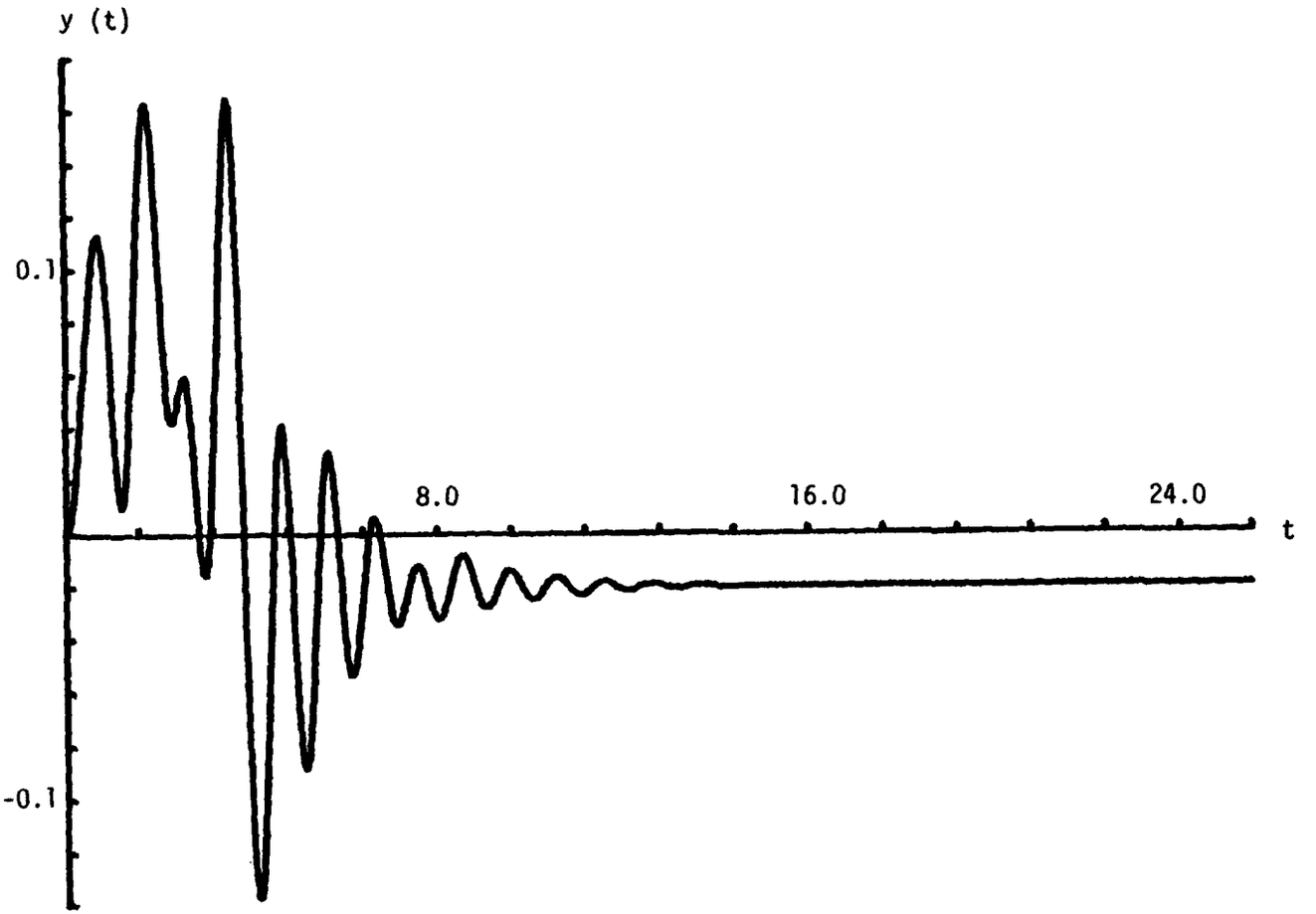

Figure 5.2. Response of Bilinear Hysteretic Structure to Input in Figure 5.1

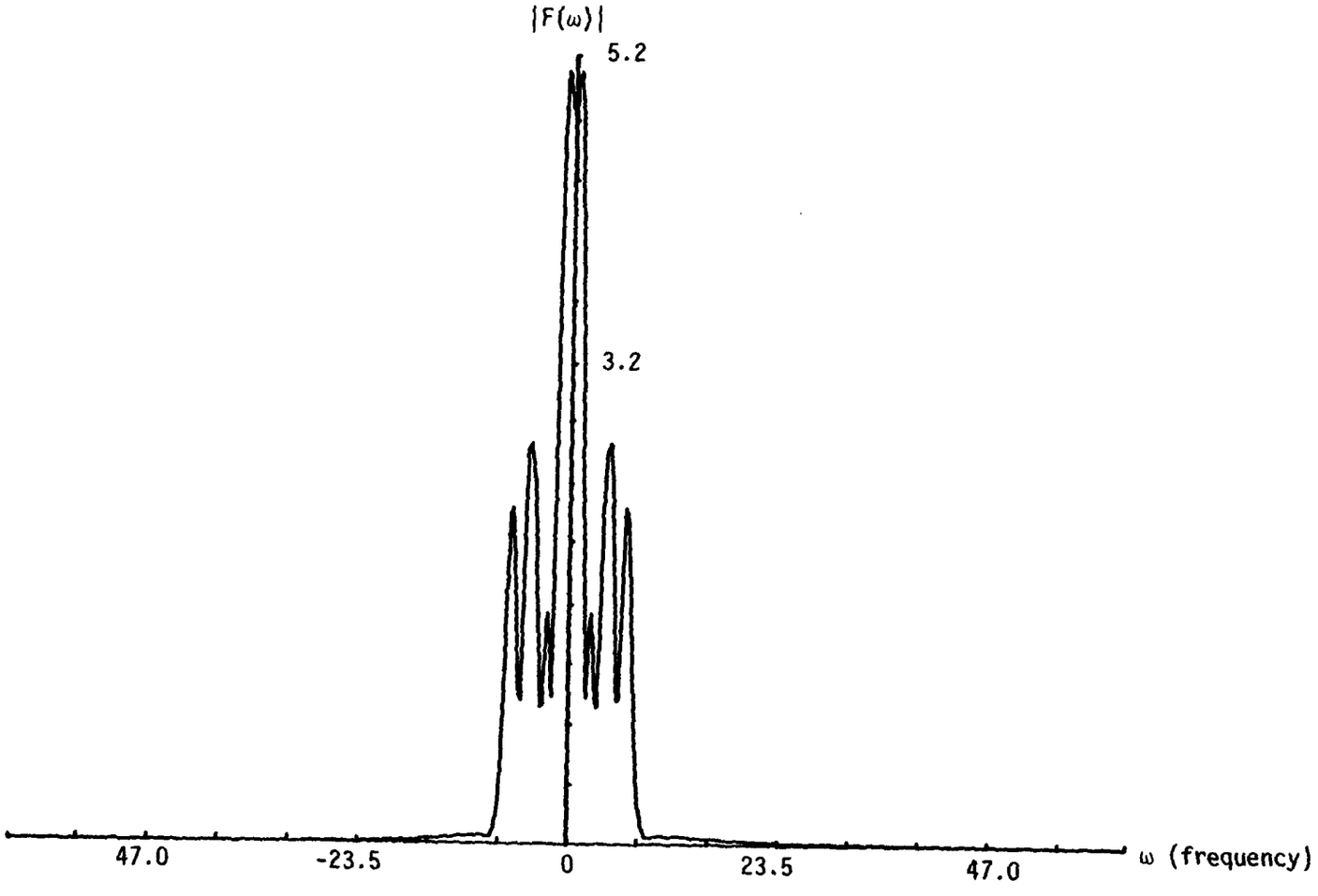

Figure 5.3. The Modulus of the Fourier Transform of the Input

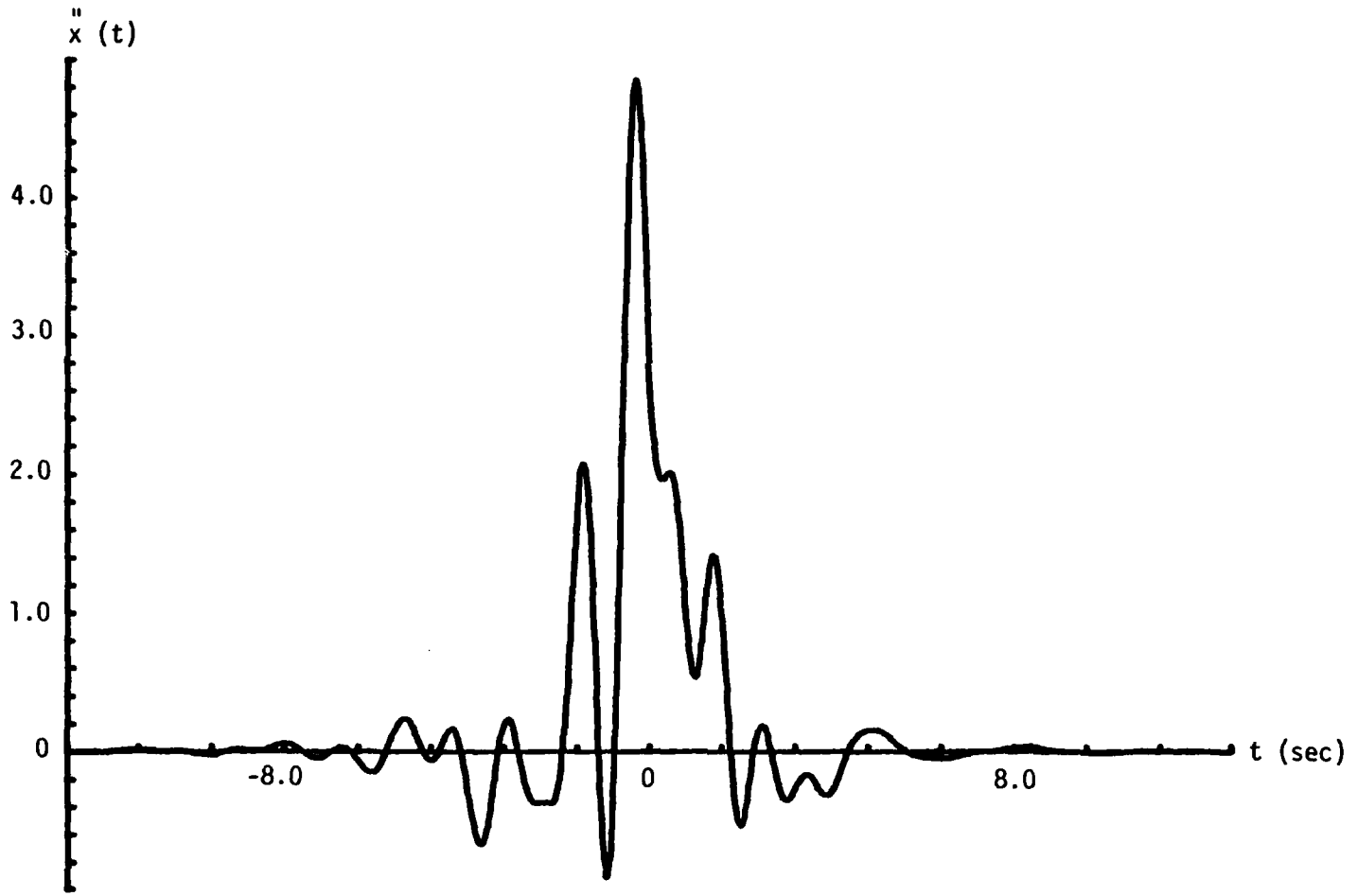

Figure 5.4. LFI Based on Maximum Displacement Criterion

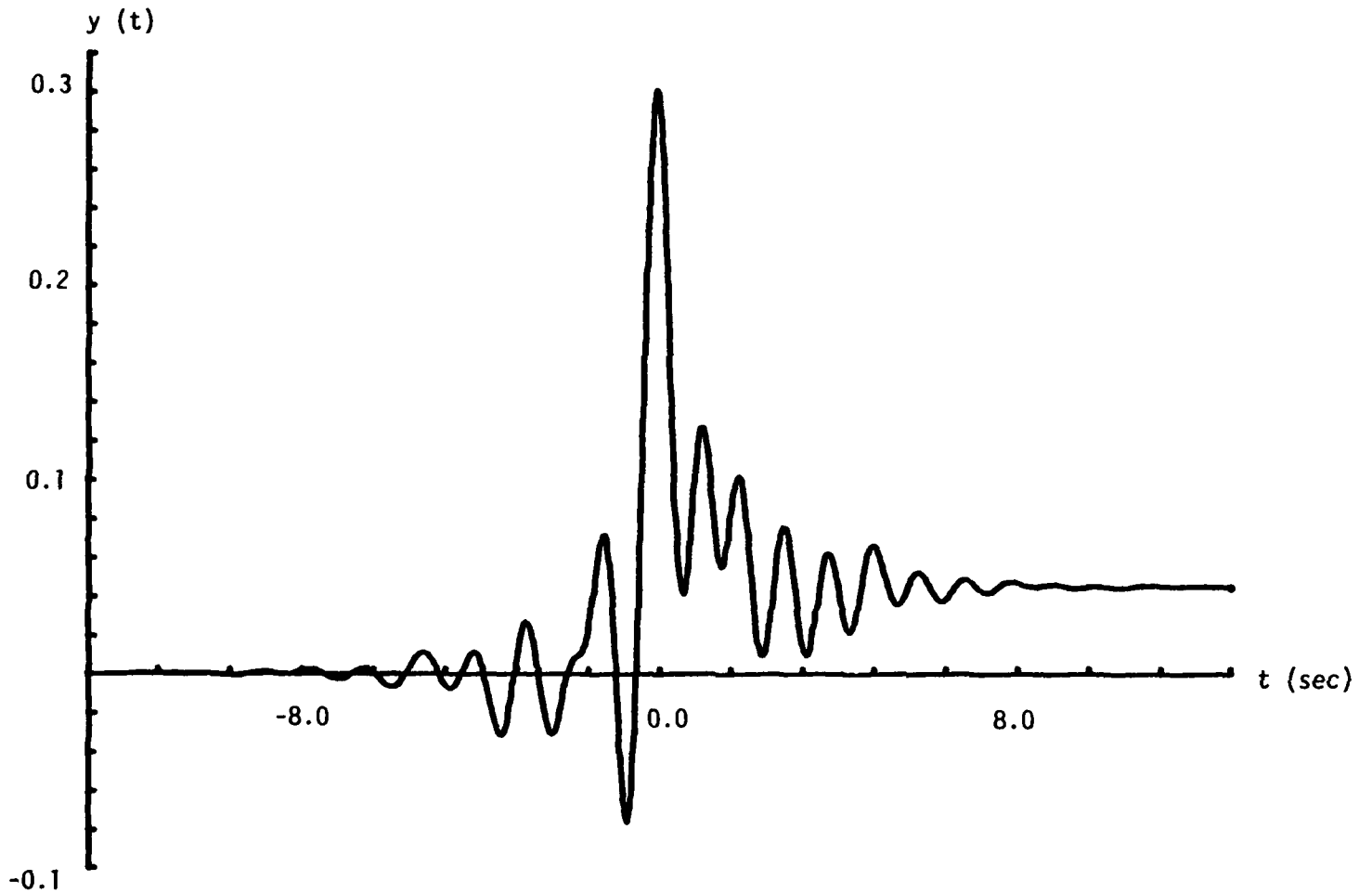

Figure 5.5 Response of Bilinear Hysteretic System to Input in Figure 5.4

the Fourier transform of the LFI are $\omega_e = 6.283$ and $\zeta_e = 0.092$. The LFI computed using Equation 3-7 is shown in Figure 5.6. The response excited by the LFI is shown in Figure 5.7. The energy dissipated during the response to the LFI is the LFR and this has magnitude 0.1871.

This example demonstrates the process used in finding the LFI and LFR of a bilinear hysteretic structure when a single input is considered.

5.2 Example Two

In this numerical example several problem sequences are solved. In order for the techniques developed in this study to be useful in the practical specification of tests, it is necessary to express the results in a form that is easy to use. Specifically, when the engineer needs to test an equipment item, it is desirable to specify a test sequence where he can run a few tests on the equipment item, and use the results to specify the LFI. The results of this numerical example will show that such a sequence can be defined.

In the first part of this example, the bilinear hysteretic structure whose parameters are given in Table 5.1 is subjected to a sequence of 16 inputs. The inputs all have the same form, Equation 5-1, and only one of the input parameters is varied; this is the amplitude. The input parameters are listed in Table 5.3, and the amplitudes for all the inputs are given. C_{ij} is the amplitude of the j^{th} frequency component of the i^{th} input.

Table 5.3. Shock Input Parameters

$N = 30$	$\alpha = 0.628$
$\omega_j = 0.1 + 0.238(j - 1)$	$j = 1,...30$
$C_{ij} = 0.2(i - 1) + 1$	$j = 1,...30, \quad i = 1,...16$

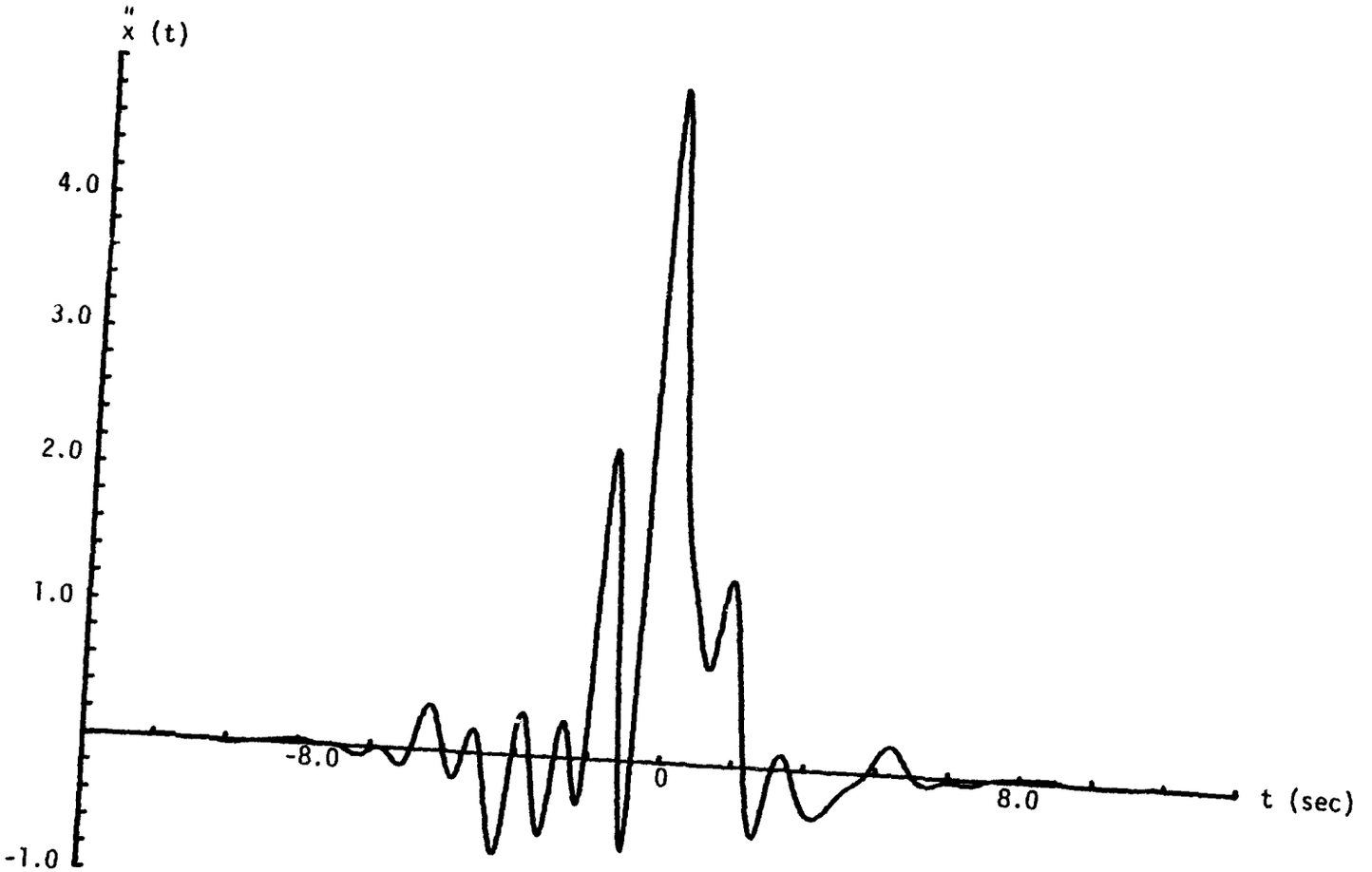

Figure 5.6. LFI Based on Maximum Energy Dissipated Criterion

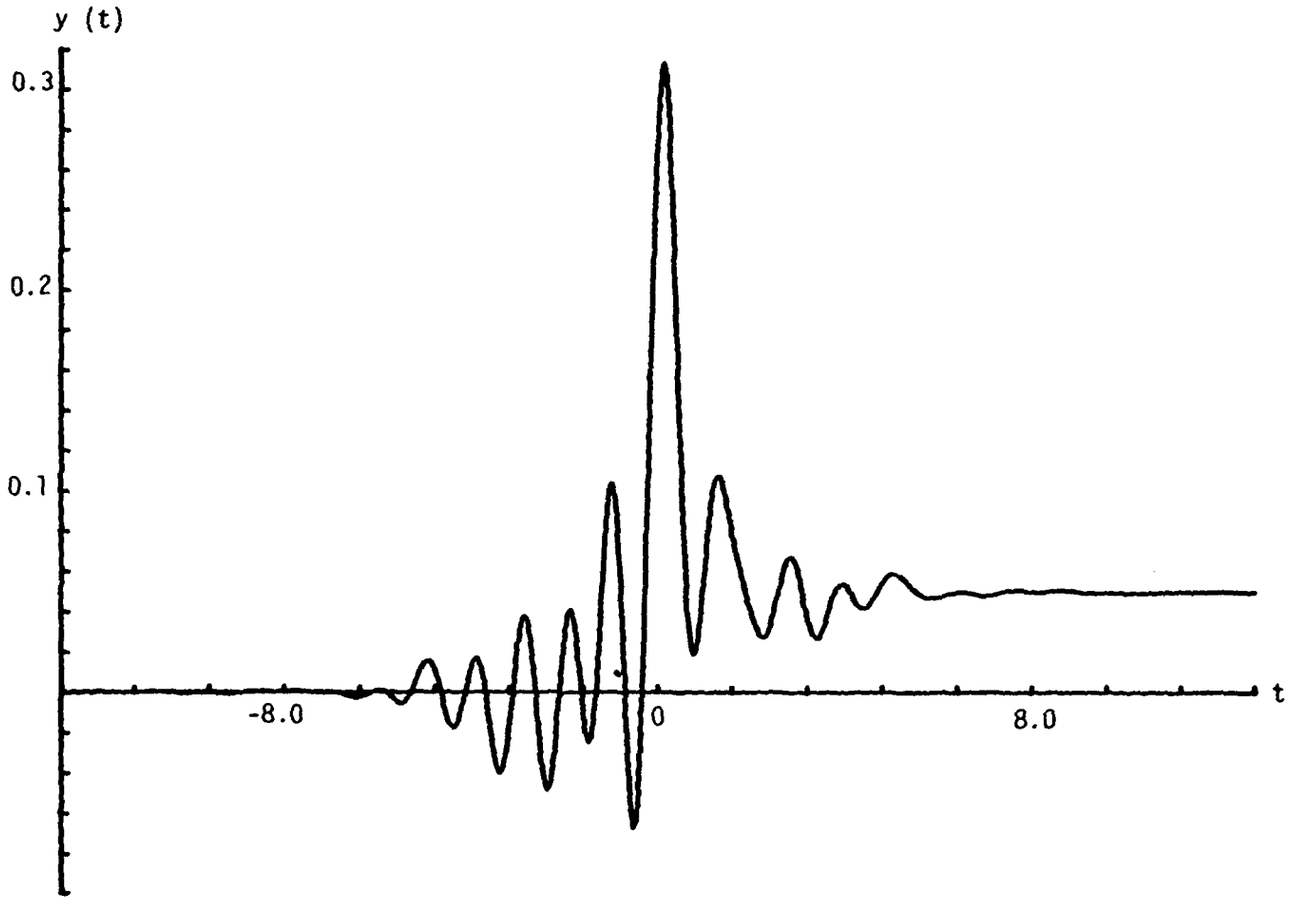

Figure 5.7. Response of Bilinear Hysteretic System to Input in Figure 5.6

The actual structural response to each input was computed. Based on the responses the actual peak displacement responses were determined. The ratio between each peak response and the yield displacement was taken to establish the ductility ratio, U, of each response. Next, the parameters of the complex phase of the Fourier transform of the LFI (using peak displacement criterion) were determined for each input. These parameters are graphed versus the ductility ratio and are shown in Figures 5.8 (ω_e parameter) and 5.9 (ζ_e parameter).

The LFR was computed for each input. This quantity was normalized by dividing by the actual maximum response, and is graphed as a function of ductility ratio in Figure 5.10.

This entire process was repeated for two more yield stiffness to elastic stiffness ratios. These are $k_y/k = 0.3$ and $k_y/k = 0.1$. The results of these analyses are also shown in Figures 5.8, 5.9, and 5.10.

All the results show the same general trends. Consider first Figure 5.8. When the ductility ratio is low, the frequency parameter changes little. As the ductility ratio increases, the frequency parameter decreases. All the curves exhibit an erratic behavior. The reason is that the inputs are random.

The plots in Figure 5.8 raise a question of interest. That is, do the curves asymptotically approach limits? The answer is probably yes, and each limit is related to the ratio between the yield stiffness and the elastic stiffness. As the structural response displacement increases far beyond the yield limit, each SDF system has a spring force versus displacement diagram that resembles a linear system response with stiffness, k_y. Since the natural frequency of an SDF system, with mass m and stiffness k, is $\sqrt{k/m}$, the parameter ω_e must approximately approach the

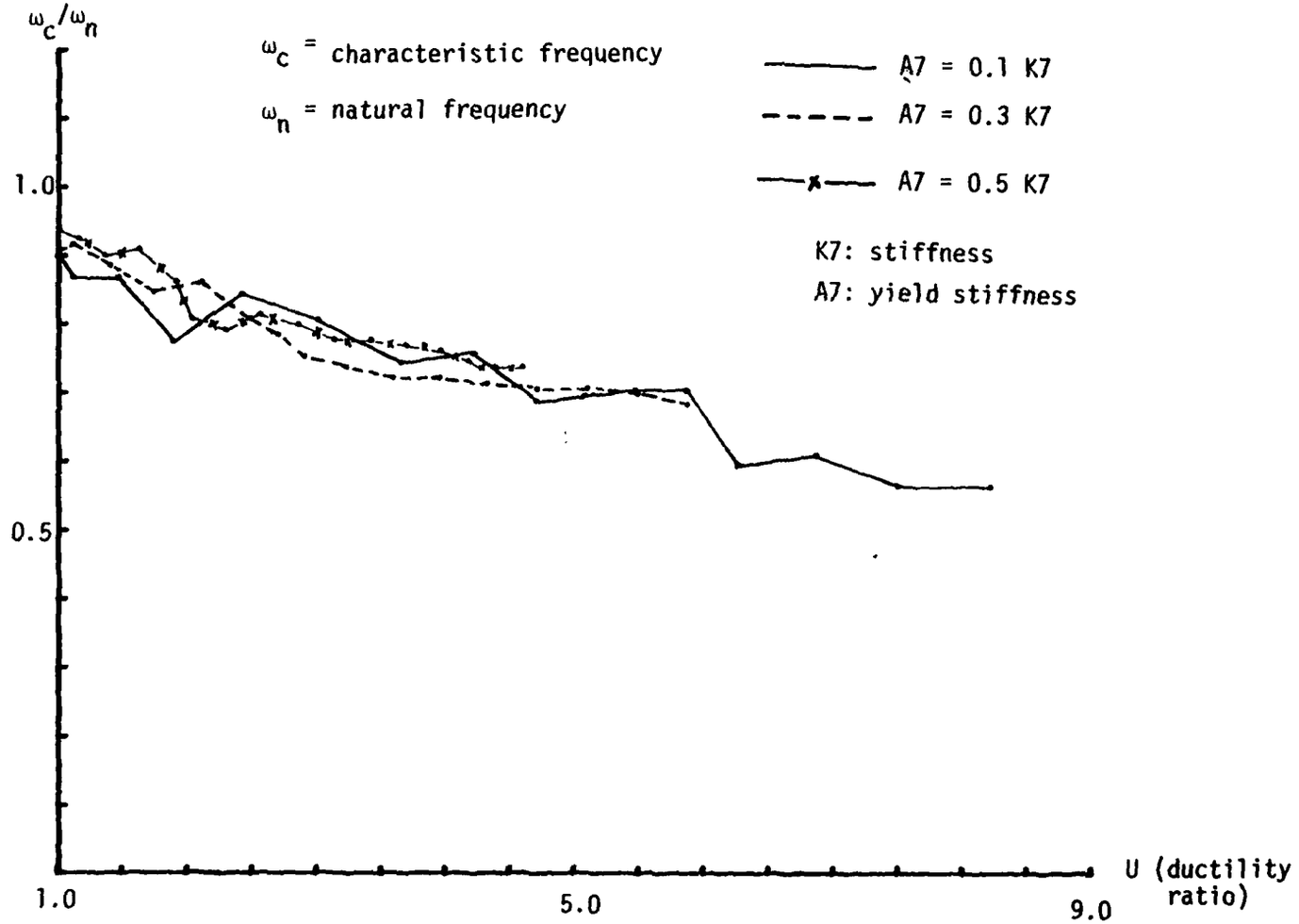

Figure 5.8. LFI Frequency Parameter versus Ductility Ratio (Displacement Criterion)

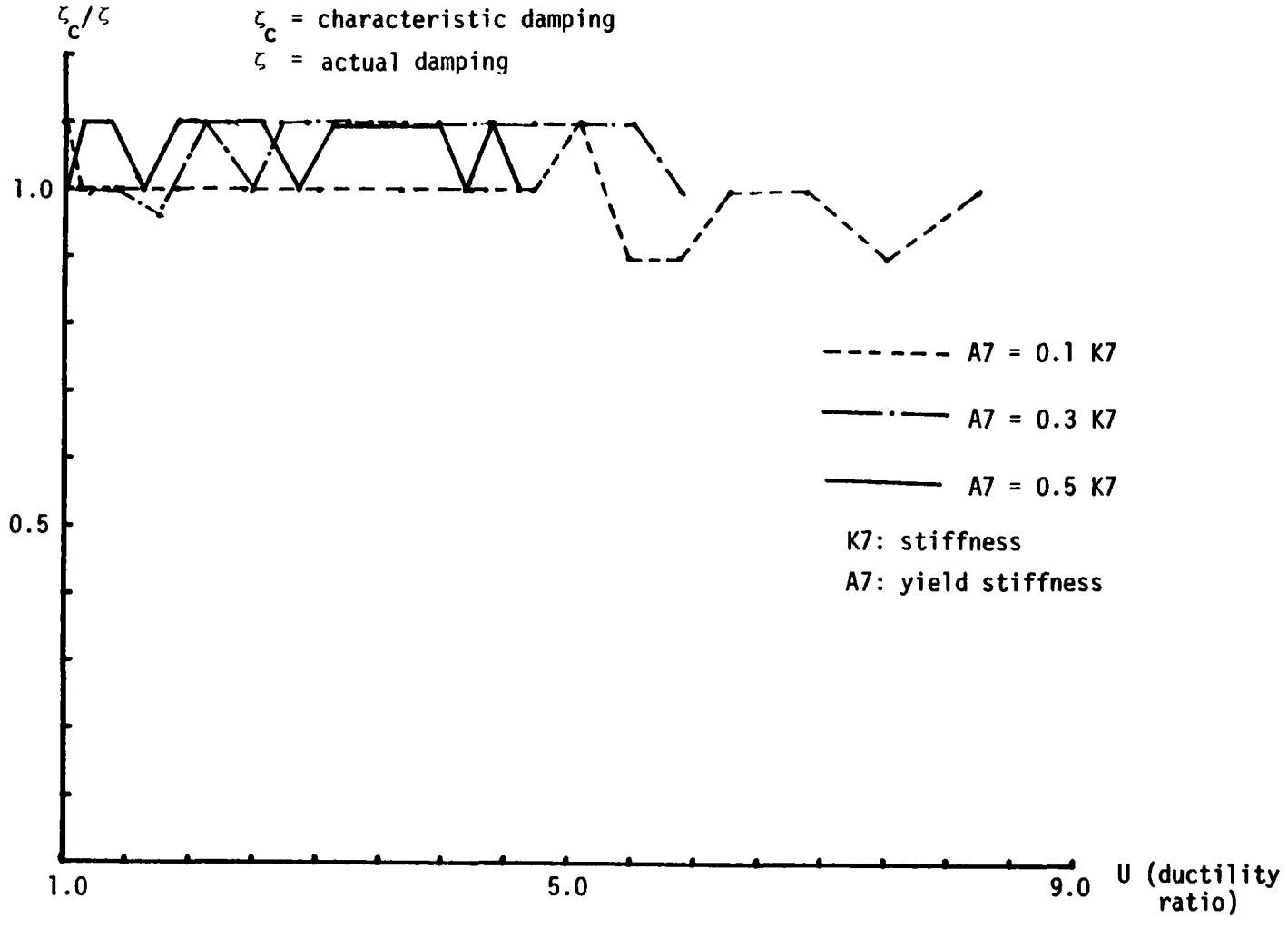

Figure 5.9. LFI Damping Parameter versus Ductility Ratio

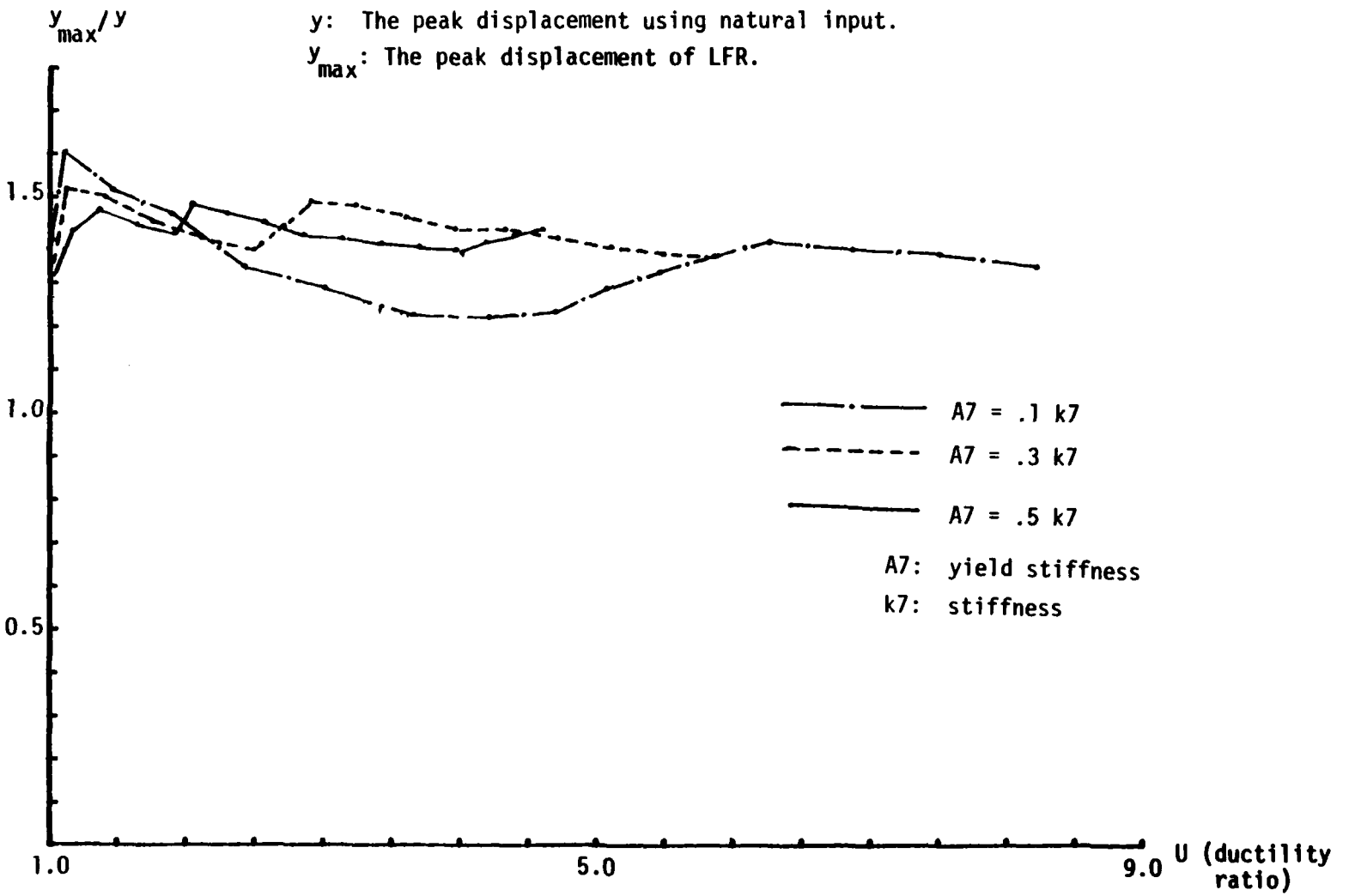

Figure 5.10. Ratio of LFR to Actual Peak Response versus Ductility Ratio

value, $\sqrt{k_y/m}$, in the limit. And the ratio ω_e/ω_n must approach $\sqrt{k_y/k}$.

An analysis was performed to establish a smooth curve for each sequence of data in Figure 5.8. Each data sequence was fitted to the mathematical model

$$\frac{\omega_e}{\omega_n} = \sqrt{\frac{k_y}{k}} + A - \frac{k_y}{k} e^{-\gamma U} \qquad (5\text{-}2)$$

where ω_e/ω_n is the ordinate of the curve, U is the abscissa, $\sqrt{k_y/k}$ is the asymptote, and A and γ were evaluated using the least squares method. The results of the analyses are given in Table 5.4.

Table 5.4. Curve Parameters for Data in Figure 5.8

$\sqrt{k_{y/k}}$	0.5	0.3	0.1
A	1.125	0.995	0.966
γ	0.572	0.226	0.112

The smooth curves are shown in Figure 5.11. The results show that the curves are relatively close to one another over the range of U values considered. This implies that the frequency parameter, ω_e, of the LFI can be chosen, approximately, even when the yield stiffness to elastic stiffness ratio is not known accurately.

Now consider Figure 5.9. Based on these curves a few statements can be made. All the curves exhibit erratic variations. The variations tend to be largest for the systems with the largest ratios of yield stiffness to elastic stiffness. There is no immediate explanation for this behavior. In any case, the damping parameter, ζ_e in the LFI appears to remain small when the damping in the actual system is small.

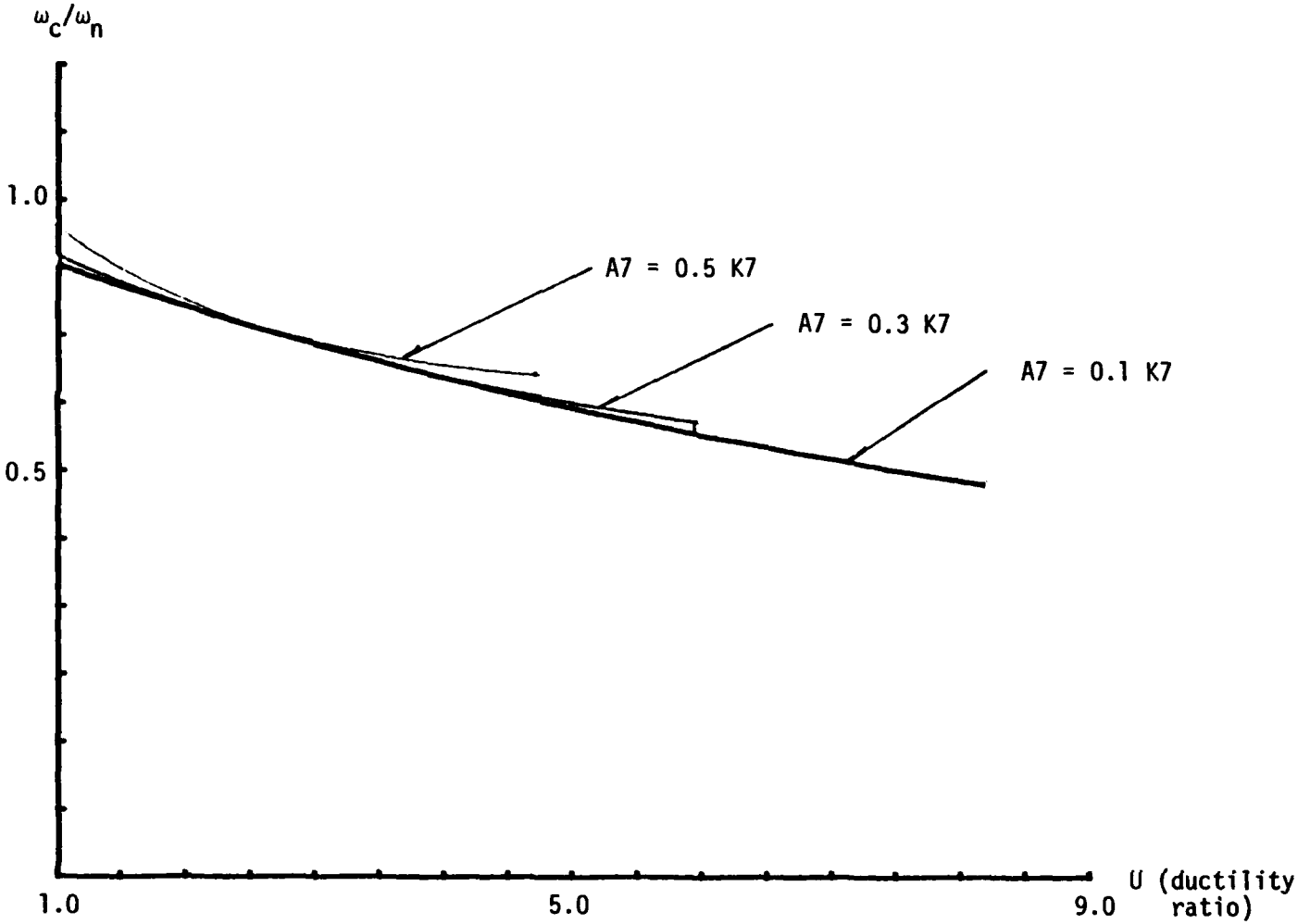

Figure 5.11. Smooth Curves Corresponding to Figure 5.8

Figure 5.10 shows that the ratio between the LFR and the actual peak response displays a certain degree of unpredictable variation. This variation is due to the fact that the inputs are random. However, the ratio appears to be constant, on the average, and the average is about 1.4. This indicates that an LFR about 40 percent greater than the actual peak response can usually be expected.

All the computations described above, in Example Two, were repeated for the case where a maximum dissipated energy criterion was used. As before, the structure whose parameters are listed in Table 5.1 was subjected to several input sequences consisting of 16 random inputs each. The inputs have the characteristics listed in Table 5.3. The actual responses were computed along with the parameters of the LFI, the LFI itself and the energy dissipated LFR. The results are shown in Figures 5.12 through 5.14.

Figure 5.12 shows the variation of the LFI frequency parameter, ω_e, with the ductility ratio of the actual input and response. Figure 5.13 shows the variation of the LFI damping parameter, ζ_e, with the ductility ratio. Figure 5.14 shows the variation of the dissipated energy LFR with the ductility ratio. The results computed using $k_y/k = 0.5$, $k_y/k = 0.3$, and $k_y/k = 0.1$ are shown.

Figure 5.12 shows that the frequency parameter of the LFI tends to remain constant with increasing ductility ratio. This result is in contrast to that obtained using the peak displacement response criterion. The three curves, representing different yield stiffness to elastic stiffness ratios, always remain near one. This indictates that the frequency parameter, ω_e in the LFI can be chosen as ω_n, regardless of the value of the yield stiffness to elastic stiffness ratio.

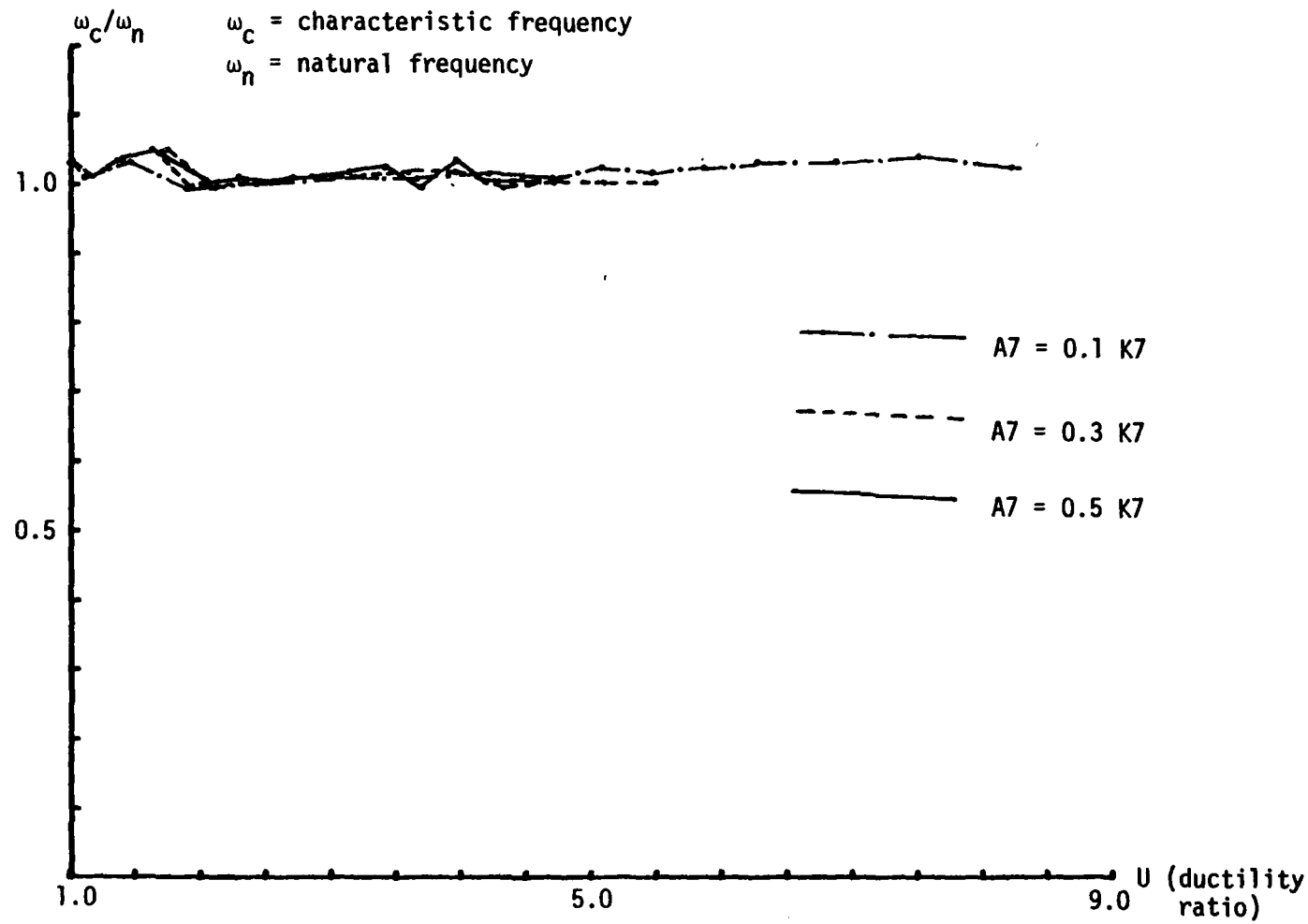

Figure 5.12. LFI Frequency Parameter versus Ductility Ratio

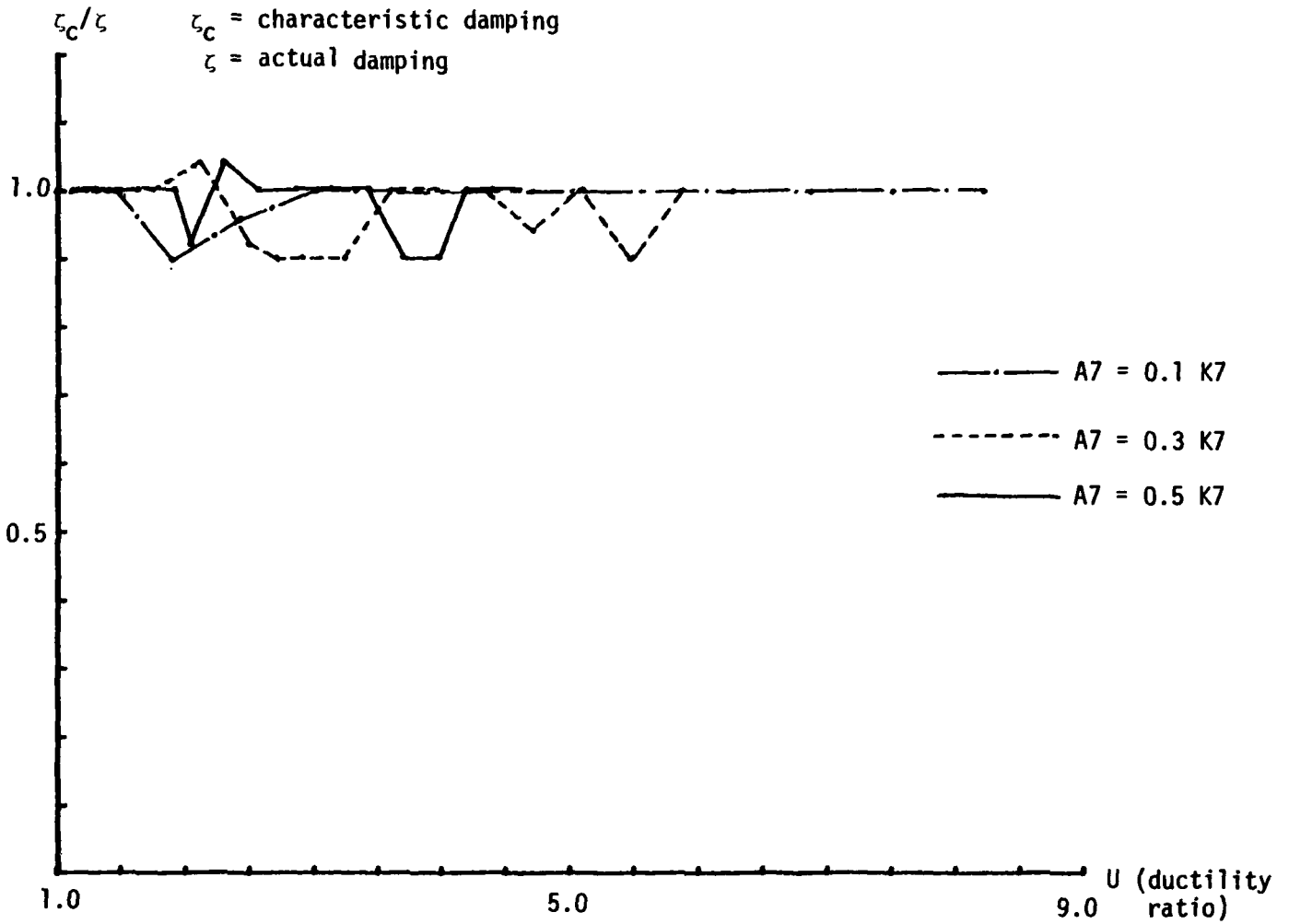

Figure 5.13. LFI Damping Parameter versus Ductility Ratio

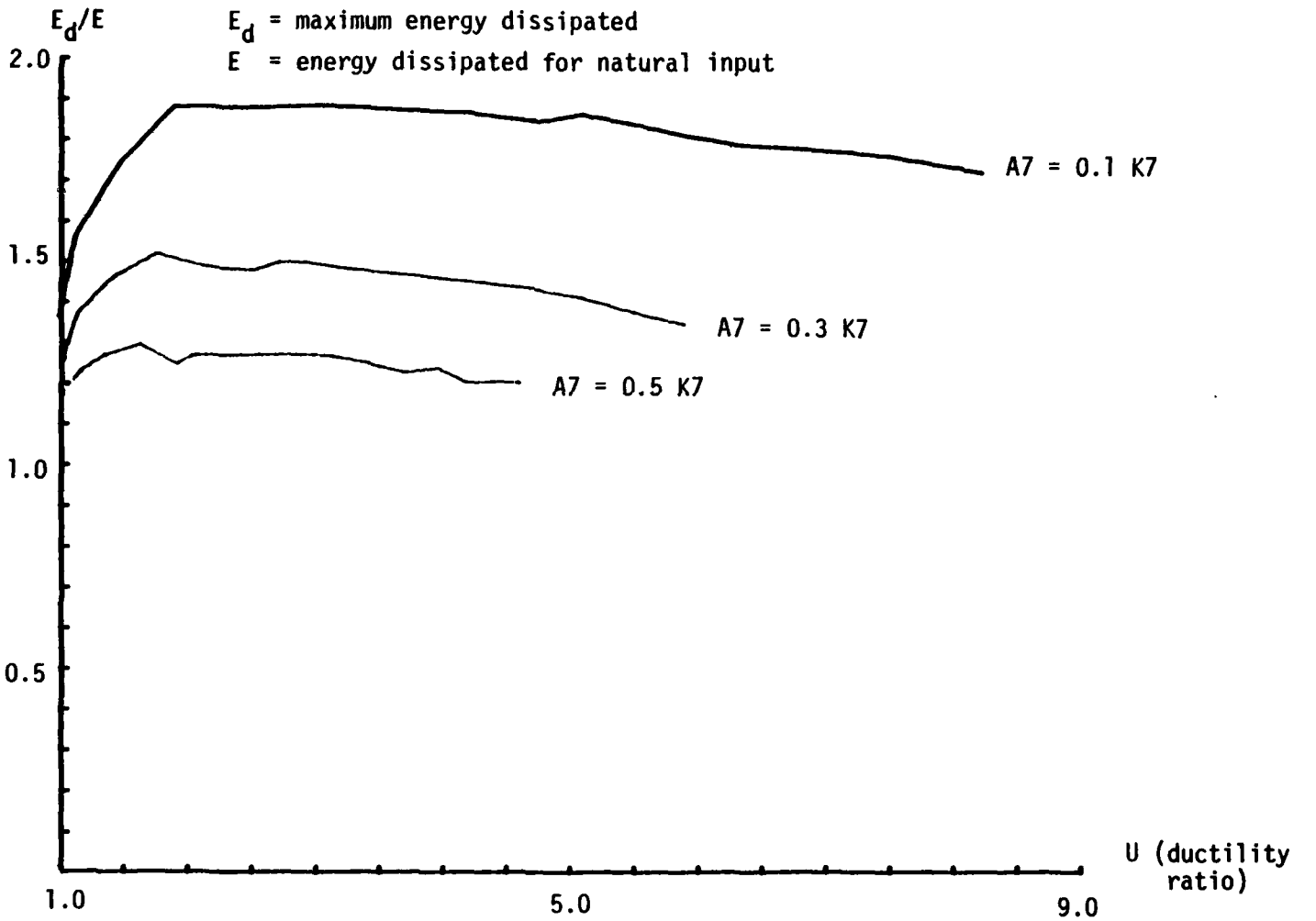

Figure 5.14. Ratio of LFR to Actual Energy Dissipated versus Ductility Ratio

Note that the frequency parameter curves obtained using the peak displacement criterion (Figure 8) are different from the frequency parameter curves obtained using the energy dissipated criterion. Therefore, the peak displacement based LFI is different from the maximum energy dissipated based LFI. To test a structure for its failure potential in the two modes, two separate tests must be run.

Figure 5.13 shows that the damping parameter in the LFI differs little from the damping parameter in the actual system. The variation is so small that the damping in the actual system can be used as the damping parameter in the LFI.

Figure 5.14 shows that the dissipated energy LFR is always greater than the energy dissipated in the actual response. The ratio of the two quantities is not constant because of the input randomness.

It was stated that the procedure outlined in this numerical example would make it easy for the test engineer to find the LFI for an equipment item. One procedure a test engineer might follow is now presented.

When an equipment item will be sujected to a class of field inputs similar in character to the input of Equation 5-1, the test engineer can specify an LFR test using a sequence of experiments. First, the test item must be instrumented. Base input is assumed, and the response at a critical point is monitored. Using a low amplitude sine sweep (or equivalent method) the fundamental frequency must be determined. The frequency response function near the fundamental frequency must be established, and this information must be used to determine the damping factor in the fundamental mode. For example, this can be inferred from the half power bandwidth.

Next, the yield point must be established. This can be done using a sequence of experiments. In each experiment the actual input is multiplied by a factor q. q is varied from a small value (say 0.05) to the value 1.0. The structure is excited using the modified input. The response at the point of interest is monitored and the peak value is determined. The values of peak response are plotted versus q. The curve generated using this approach remains linear until yielding occurs. After yielding, the slope of the curve diminishes. The value of q corresponding to the yield point and the peak value of the response where the yield displacement is realized can be determined from the curve.

Now the test engineer applies the actual input to the equipment item and observes the peak value of the response at the point of interest. The ratio between this quantity and the peak value of the response where yielding first occurs is the ductility ratio. This ductility ratio can be used to enter Figures 5.8 and 5.12 (or 5.11 and 5.12) to determine the frequency parameters for the displacement and dissipated energy LFIs.

The test engineer determines the modulus of the Fourier transform of the actual input, then uses this with frequency parameter given above and the actual system damping factor to establish the LFIs. The test input is computed using the above information in Equations 3-6 and 3-7.

The technique described above can be used to establish the LFI parameters for other classes of random inputs. The analysis sequence is simply repeated using the other input in place of Equation 5-1.

6.0 Summary and Conclusion

The objective of this paper was to establish a method to search for a test input that excites a conservative response in an equipment item capable of inelastic response. A method for specifying a conservative test input based on measured field inputs was established. The criteria of peak displacement response and energy dissipated were used.

The technique developed here was based on the linear theory of least favorable response (LFR). It was assumed that when an equipment item is subjected to a severe excitation, the response may be inelastic. An equipment item executing inelastic response displays a diminished stiffness. Therefore, the characteristic frequency of an inelastic structure is lower than its fundamental frequency. This study specified a method to search for the input that causes the inelastic system response to be a maximum. The input has the same form as the linear least favorable input (LFI).

Equations 3-6 and 3-7 establish the form of the LFI. The intensity of the actual shock input is accurately reflected in the test since the LFI preserves the modulus of the Fourier transform of the acutal input. Comparison of Figures 5.1 and 5.4 shows that the general character of the actual input is preserved in the LFI.

The potential for inelastic response is accounted for in this study since Equation 3-4 is assumed to govern the response of the systems under consideration.

Example one demonstrates how the techniques developed in this investigation can be applied in the definition of an actual test input. Example two shows that the results can be generalized for easy application in the specification of test inputs.

Some important results of this study are shown in Figures 5-8 and 5-12. These show the frequency parameter to be used in specification of an LFI as a function of ductility ratio. The numerical investigtions show that the frequency parameter is the most important factor in the definition of the displacement criterion LFI. Figures 5-8 permits the easy identification of this parameter for test definition.

The damping which corresponds to the maximum displacement response and maximum energy dissipated was also determined. The damping variation is shown in Figures 5-9 and 5-13. It is concluded from the computations that the change of damping does not significantly affect the LFR. Hence, it is recommended that the damping parameter in the LFI be defined as the damping in the actual system.

The procedures developed in this study can be useful in practical applications. Exampe Two showed that a procedure can be developed to specify the parameters of an LFI, when only the general form of the actual input and the ductility ratio of the actual response are known. The procedure developed in Example Two can be simplified even further. For example, note that the LFI depends not on the form of the actual input, but rather on the complex modulus of the Fourier transform of the input. In view of this, the frequency parameters of the LFI can be written as a function of the ductility ratio for an input whose Fourier transform modulus has certain characteristics, such as "increasing with frequency near ω_n," or "decreasing with frequency near ω_n," or "constant with frequency near ω_n." Using this approach the parameters of an LFI would not be tied to a specific input form, but rather to an input whose Fourier transform modulus has a specific form. Other simplifications and generalizations may also be possible.

The results obtained during this investigation are limited by the assumptions of the study. Most important, only single-degree-of-freedom, bilinear hysteretic systems were studied. Further, random inputs were used, but the probabilistic character of the response was not investigated. Only one form for the LFI was used.

Future studies may seek to improve the present analyses in several areas. For example, an alternate form for the LFI may be sought; specifically, inputs which generate more severe responses may be developed. Other forms of inelastic behavior may be considered. Probabilistic studies may be performed; these can be used to predict the probability of conservatism of a shock test. Most important, a shock test specification procedure which explicitly accounts for the characteristics of inelastic multi-degree-of-freedom systems must be pursued.

REFERENCES

1. Matsuzaki, Yuji, "A Review of Shock Response Spectrum," The Shock and Vibration Digest, 9(3), pp. 3-12, March 1977.

2. Morrone, A., "Analysis of Seismic Testing Motions with Instantaneous Response Spectra," Nuclear Engineering and Design, 51,(3), pp. 445-451, February 1979.

3. Nelson, F. C., "Shock and Seismic Excitation of Mechanical Equipment," ASME Paper 74-DE-3, Presented at the Design Engineering Conference and Show, Chicago IL, April 1-4, 1974.

4. Hadjian, A. H., "Seismic Response of Structures by the Response Spectrum Method," Nuclear Engineering and Design, 66, pp. 179-207, 1981.

5. Trubert, M., and Salama, M., "Generalized Modal Shock Spectra Method for Spacecraft Loads Analysis," AIAA Journal, 18(8), pp. 988-994, August 1980.

6. Drenick, R. F., "Model Free Design of Aseismic Structures," Journal of the Engineering Mechanics Division, Proceedings, ASCE, 96, pp. 483-493, August 1970.

7. Shinozuka, M., "Maximum Structural Response to Seismic Excitations," Journal of the Engineering Mechanics Division, Proceedings ASCE, 96, pp. 483-493, August 1970.

8. Witte, A. F., and Wolf, R. J., "Comparison of Shock Spectrum Techniques and the Method of Least Favorable Response," The Shock and Vibration Bulletin, Bulletin 44, Part 3, pp. 7-24, August 1974.

9. Paez, Thomas L., "Conservatism in Least Favorable Response Analysis and Testing," The Shock and Vibration Bulletin, Bulletin 51, Part 2, pp. 93-109, May 1981.

10. Youssef, N. A. N., and Popplewell, N., "A Theory of the Greatest Maximum Response of Linear Structures," Journal of Sound and Vibration, 56(1), pp. 21-33, 1978.

11. Youssef, N. A. N., and Popplewell, N., "The Maximax Response of Discrete Multi-Degree-of-Freedom Systems, Journal of Sound and Vibration, 64(1), pp. 1-15, 1979.

12. Popplewell, N., and Youssef, N. A. N., "A Comparison of Maximax Response Estimates, Journal of Sound and Vibration, 62(3), pp. 339-352, 1979.

13. Populis, A., "Maximax Response with Input Energy Constraints and the Matched Filter Principle," IEEE Transactions on Circuit Theory, 17(2), pp. 175-182, May 1970.

14. Baca, Thomas Joseph, Characterization of Conservatism in Mechanical Shock Testing of Structures, Ph.D. Dissertation, Stanford University, Stanford, CA, September 1982.

15. Kawakatsu, T., Kitade, K., Takemori, T., Kuwabara, Y., and Ogiwara, Y., "Floor Response Spectra Considering Elasto-Plastic Behavior of Nuclear Power Facilities," Paper K9/4, Transactions of the International Conference on Structural Mechanics in Reactor Technology, 5th, K(b): Seismic Response Analysis of Nuclear Power Plant Systems, Berlin, Germany, August 13-17, 1979.

16. Mahin, Stephen A., and Bertero, Vitelmo V., "An Evaluation of Inelastic Seismic Design Spectra," Journal of the Structural Division, Proceedings ASCE, 107(ST9), pp. 1777-1795, September 1981.

17. Iwan, W. D., "Estimating Inelastic Response Spectra from Elastic Spectra,"Earthquake Engineering and Structural Dynamics, 8, pp. 375-388, 1980.

18. Paez, T., Wang, M. L., Ju, F. D., "Diagnosis of Damage in SDF Structures," Report No. CE-60(82) AFOSR-993-1, Bureau of Engineering Research, The University of New Mexico, Albuquerque, March 1982.

19. Ang, A. H. S., Wen, Y. K., "Prediction of Earthquake Damage under Random Earthquake Excitation," Earthquake Ground Motion and Its Effects on Structures, AMD Vol. 53, ASME, November 1982.

20. Wang, M. L., Paez, T. L., Ju, F. D., "Mathematical Models for Damageable Structures," to be published as Bureau of Engineering Research Report, The University of New Mexico, Albuquerque, March 1983.

21. Clough, R. W., Penzien, J., Dynamics of Structures, McGraw-Hill, Inc., New York, 1975.

22. Yao, J. T. P., Toussi, S., Sozen, M. A., "Damage Assessment from Dynamic Response Measurements," Proceedings of the Ninth U.S. National Congress of Applied Mechanics, Cornell Univ., June 21-25, 1982.

23. Ishizaka, M., Fu, K. S., Yao, J. T. P., "Computer Based Systems for the Assessment of Structural Damage," IABSE Colloquium on Informatics in Structural Engineering, Bergamo, Italy, October 6-8, 1982.


FILM